



Review

# A Review of the Current Landscape of SARS-CoV-2 Main Protease Inhibitors: Have We Hit the Bullseye Yet?

Guillem Macip , Pol Garcia-Segura , Júlia Mestres-Truyol, Bryan Saldivar-Espinoza, Gerard Pujadas \* and Santiago Garcia-Vallvé \*

Research Group in Cheminformatics & Nutrition, Departament de Bioquímica i Biotecnologia, Campus Sescelades, Universitat Rovira i Virgili, 43007 Tarragona, Catalonia, Spain; guillem.macip@gmail.com (G.M.); polgarse2@gmail.com (P.G.-S.); juliamt110@gmail.com (J.M.-T.); bsaldivar.emc2@gmail.com (B.S.-E.)

\* Correspondence: gerard.pujadas@gmail.com (G.P.); santi.garcia-vallve@urv.cat (S.G.-V.)

**Abstract:** In this review, we collected 1765 severe acute respiratory syndrome coronavirus 2 (SARS-CoV-2) M-pro inhibitors from the bibliography and other sources, such as the COVID Moonshot project and the ChEMBL database. This set of inhibitors includes only those compounds whose inhibitory capacity, mainly expressed as the half-maximal inhibitory concentration ( $IC_{50}$ ) value, against M-pro from SARS-CoV-2 has been determined. Several covalent warheads are used to treat covalent and non-covalent inhibitors separately. Chemical space, the variation of the  $IC_{50}$  inhibitory activity when measured by different methods or laboratories, and the influence of 1,4-dithiothreitol (DTT) are discussed. When available, we have collected the values of inhibition of viral replication measured with a cellular antiviral assay and expressed as half maximal effective concentration ( $EC_{50}$ ) values, and their possible relationship to inhibitory potency against M-pro is analyzed. Finally, the most potent covalent and non-covalent inhibitors that simultaneously inhibit the SARS-CoV-2 M-pro and the virus replication in vitro are discussed.

**Keywords:** COVID-19; M-pro inhibitors; 3CL-pro inhibitors; computational chemistry; protease inhibitors; virtual screening



**Citation:** Macip, G.; Garcia-Segura, P.; Mestres-Truyol, J.; Saldivar-Espinoza, B.; Pujadas, G.; Garcia-Vallvé, S. A Review of the Current Landscape of SARS-CoV-2 Main Protease Inhibitors: Have We Hit the Bullseye Yet? *Int. J. Mol. Sci.* **2022**, *23*, 259. <https://doi.org/10.3390/ijms23010259>

Academic Editors: Francesco Caruso and Miriam Rossi

Received: 3 December 2021

Accepted: 25 December 2021

Published: 27 December 2021

**Publisher's Note:** MDPI stays neutral with regard to jurisdictional claims in published maps and institutional affiliations.



**Copyright:** © 2021 by the authors. Licensee MDPI, Basel, Switzerland. This article is an open access article distributed under the terms and conditions of the Creative Commons Attribution (CC BY) license (<https://creativecommons.org/licenses/by/4.0/>).

## 1. Introduction

Since the onset of the COVID-19 pandemic, the scientific community has focused on studying the severe acute respiratory syndrome coronavirus 2 (SARS-CoV-2) virus that causes the disease and on developing therapies and vaccines, several of which have been developed in record time. In the pharmacological field, no drugs have yet been definitively approved to inhibit the replication of SARS-CoV-2 and stop the development of COVID-19. Several targets are being studied, including the main protease (M-pro), which plays an essential role in virus replication [1]. This protease and the papain-like protease cleave the pp1a and pp1ab polyproteins to produce several nonstructural proteins, including M-pro itself, required for virus replication and transcription [1]. The high conservation of M-pro among related viruses, the importance of M-pro in the replication of the virus and the fact that M-pro only exists in coronaviruses and not in humans makes it an attractive target for the development of antiviral drugs [2–4]. SARS-CoV-2 M-pro has 306 amino acids that form three domains (I, II and III) [4]. The M-pro binding site is located between domains I and II, and domain III is involved in dimerization, which is essential for M-pro activity [4]. Similar to the M-pro from SARS-CoV-1 and other coronaviruses, SARS-CoV-2 M-pro has two catalytic amino acids, His41 and Cys145 (Figure 1). A catalytic water molecule is also important and makes a strong hydrogen bond with His41 [5]. Although some allosteric binding sites have been identified for the SARS-CoV-2 M-pro [6–9], most of the inhibitors crystallized within the M-pro bind to the active site [10]. One strategy used to find SARS-CoV-2 M-pro inhibitors, especially at the beginning of the pandemic, was

drug repositioning [2,11–13]. This strategy is based on looking for drugs approved for one disease (therefore, its safety and possible adverse effects are known) that can be used to treat another—in this case, COVID-19. One of the most widely used computational tools for repositioning drugs, or looking for compounds with new activities, is what is known as protein-ligand docking. This tool predicts whether a particular molecule can bind (and, if it can, how) to a particular target (for example, the SARS-CoV-2 M-pro [14]). However, protein-ligand docking has several limitations, such as the consideration of the protein as a rigid body and the lack of confidence in the ability of scoring functions to give accurate binding energies [15,16]. In addition, the flexibility of the SARS-CoV-2 M-pro makes it a challenging target for small-molecule inhibitor design [17]. Using two different SARS-CoV-2 M-pro structures and five protein-ligand docking methods, we have recently shown that docking scores or the Gibbs free energy ( $\Delta G$ ) calculated with an MM-GBSA method [18] do not correlate with bioactivity [19], probably because of the inability of common docking programs to correctly reproduce the binding modes of SARS-CoV-2 M-pro inhibitors [20]. This reinforces the idea that it is essential to validate the results obtained by protein-ligand docking or any other computational tool, especially when analyzing SARS-CoV-2 M-pro inhibitors [19,21–23]. The results of protein-ligand docking can be computationally validated by re-docking, cross-docking and applying the same protocol to a set of known active compounds and a set of decoy or inactive compounds [19]. Protein-ligand docking is expected to discriminate decoys from active compounds. If docking scores are used to rank the potency of a set of compounds, it must first be demonstrated that there is a correlation between docking scores and activity or potency, for example, expressed as  $IC_{50}$  values [19]. However, the best way to validate the predictions of protein-ligand docking is to experimentally test the predicted bioactivity of selected hits.

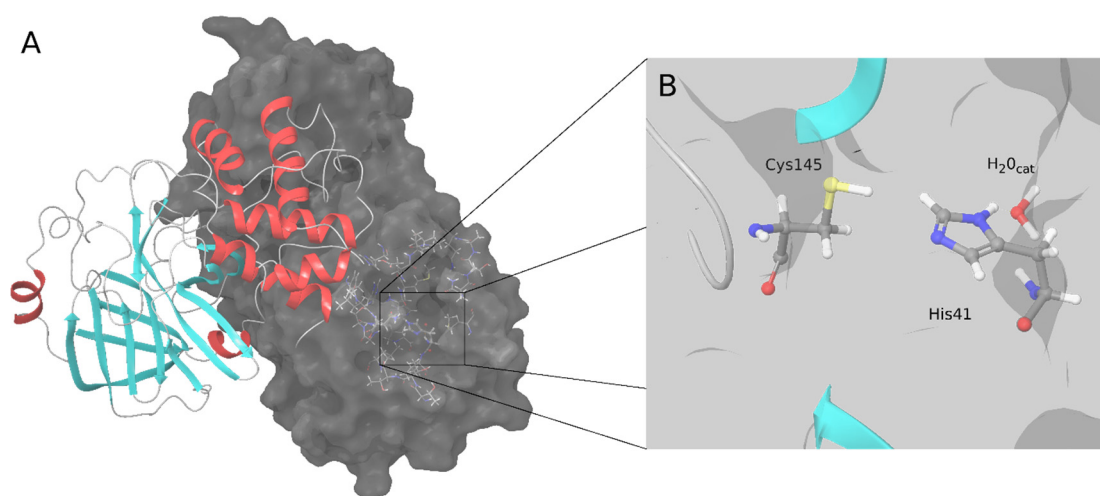


**Figure 1.** SARS-CoV-2 M-pro structure. (A) Biological assembly of the M-pro in its dimeric form. The left protomer is shown in cartoon representation, colored by protein secondary structure, and the right protomer is displayed as a surface. (B) Detailed snapshot of the catalytic water, Cys145 and His41.

Since the beginning of the COVID-19 pandemic, developing SARS-CoV-2 M-pro inhibitors has been an active area of research. However, it did not have to start from scratch. Previous research about protease inhibitors, especially from SARS-CoV and MERS-CoV, proved to be useful [24,25]. Known inhibitors of proteases from HIV and Hepatitis C virus, in addition to calpain and caspase-3 inhibitors, were systematically analyzed to test their capacity to inhibit the SARS-CoV-2 M-pro [26]. Compounds developed against the M-pro of other coronaviruses were also tested, and some were found to be potent SARS-CoV-2 M-pro inhibitors [24,27,28]. The complete genome sequence of SARS-CoV-2 [29] and the first crystallized structure of the SARS-CoV-2 M-pro [4] were two important

milestones in the development of new SARS-CoV-2 M-pro inhibitors. The article describing the first crystallized SARS-CoV-2 M-pro structure (the 6LU7 structure) also presented the first SARS-CoV-2 M-pro inhibitors [4]. These first inhibitors included the N3 compound, which had previously been developed as a protease inhibitor for multiple coronaviruses, including SARS-CoV and MERS-CoV, approved drugs (such as disulfiram and carmo-fur) and preclinical or clinical-trial drug candidates (ebselen, shikonin, tideglusib, PX-12 and TDZD-8) [4]. Since then, thousands of compounds have been suggested as SARS-CoV-2 M-pro inhibitors through computational methods such as protein-ligand docking, high-throughput screening experiments, computer-aided design and synthesis of new compounds. Several articles have reviewed the SARS-CoV-2 M-pro inhibitors discovered to date [25,28,30–38]. In this review, we collected 1765 SARS-CoV-2 M-pro inhibitors from the bibliography and other sources such as the COVID Moonshot project [39,40] and the ChEMBL release 29 database [41]. This set of inhibitors includes only those compounds whose inhibitory capacity, mainly expressed as the half-maximal inhibitory concentration ( $IC_{50}$ ) value, against M-pro from SARS-CoV-2 has been determined. We did not include compounds predicted only by docking or other computational tools. As we have discussed previously, to avoid false positives and false negatives, the results of automated protein-ligand docking should not be used as the only evidence to predict SARS-CoV-2 M-pro inhibitors [19]. Several covalent warheads are used to treat covalent and non-covalent inhibitors separately. Chemical space, the variation of the  $IC_{50}$  inhibitory activity when measured by different methods or laboratories and the influence of 1,4-dithiothreitol (DTT) are discussed. When available, virus replication inhibition values, measured with a cellular antiviral assay, were collected, and their relationship with the inhibitory potency against M-pro is shown. Finally, the most potent inhibitors that simultaneously inhibit the SARS-CoV-2 M-pro and the virus replication in vitro are discussed.

## 2. SARS-CoV-2 M-Pro Inhibitors

Table 1 shows the origin of the non-redundant set of 1765 SARS-CoV-2 M-pro inhibitors collected (see supplementary file S1). This set of inhibitors includes only those compounds whose inhibitory capacity, mainly expressed as the  $IC_{50}$  value, against M-pro from SARS-CoV-2 has been determined. A total of 758 compounds were extracted from peer-reviewed articles published between January 2020 and August 2021. When multiple  $IC_{50}$  values were found for the same compound, the mean value was calculated. From a set of 1037 M-pro inhibitors with an  $IC_{50}$  value downloaded from the COVID Moonshot project [39,40] on 1st October 2021, the compounds that had already been collected from the bibliographic search were discarded. In the end, 999 compounds were collected from COVID Moonshot. The  $IC_{50}$  values of these compounds were estimated as the mean value of the  $IC_{50}$  values from two biochemical assays: a fluorescence-based assay and a Rapid-Fire Mass Spectrometry assay. Finally, 8 compounds were collected from the ChEMBL database [41], which contained more SARS-CoV-2 M-pro inhibitors, but most of them had already been collected from the bibliography. The SMILES of the 1765 SARS-CoV-2 M-pro inhibitors were standardized with the Standardizer 21.15.0 program from ChemAxon (<http://www.chemaxon.com>, accessed on 4 September 2021). The  $pIC_{50}$  values of the SARS-CoV-2 M-pro inhibitors collected range from 2.5 to 9.0 (Table 1). Putative covalent inhibitors were identified by the presence of typical covalent warheads (Table 2). When one of these warheads is in the appropriate position within the M-pro binding site, it can form a covalent bond, usually with the catalytic Cys145 [25]. There are twice as many non-covalent inhibitors as putative covalent inhibitors (Table 1), although  $pIC_{50}$  values are highest in some putative covalent inhibitors (Table 1 and Figure 2). However, conventional  $IC_{50}$  measurements are of limited value for characterizing the potency of irreversible covalent inhibitors, because incubation for different periods of time would provide different  $IC_{50}$  values [42]. Other parameters, such as molecular weight, LogP, number of hydrogen bond donors and hydrogen bond acceptors were similar between the covalent and non-covalent sets (see Supplementary Figure S1).

**Table 1.** Number of SARS-CoV-2 M-pro inhibitors collected.

SARS-CoV-2 M-Pro Inhibitor Set	Number of Compounds (Covalent/Non-Covalent) <sup>1</sup>	pIC <sub>50</sub> Range	pIC <sub>50</sub> Range Covalent	pIC <sub>50</sub> Range Non-Covalent
From the bibliography	758 (346/412)	2.5–9.0	3.4–9.0	2.5–8.3
From COVID Moonshot	999 (205/794)	4.0–7.8	4.0–7.8	4.0–7.4
From ChEMBL	8 (1/7)	5.4–6.1	5.4	5.5–6.1
All	1765 (552/1213)	2.5–9.0	3.4–9.0	2.5–8.3

<sup>1</sup> Putative covalent and non-covalent inhibitors were identified by the presence or absence of the covalent warheads shown in Table 2.

**Table 2.** Covalent warheads that can be used to identify putative covalent inhibitors. It shows the SMARTS that can be used to identify each warhead and some examples of SARS-CoV-2 inhibitors that contain each warhead. These covalent warheads were used to identify putative covalent inhibitors among the known SARS-CoV-2 M-pro inhibitors.

Warhead	SMARTS	Examples
Acrylamide	[C;H2:1]=[C;H1]C(N)=O	CVD-0004255
Chloroacetamide	Cl[C;H2:1]C(N)=O	BFC204
Vinylsulfonamide	NS(=O)([C;H1]=[C;H2:1])=O	
Nitrile	N#[C:1]-[*]	Isavuconazole
Michael acceptors	C=!@CC=[O,S]	Cinanserin, MPI2, MPI9, N3
Alpha-ketoamide	C(=O)(C=O)N	Boceprevir, narlaprevir, telaprevir, UAWJ248
Aldehyde	[CX3H1](=O)	GC373, MI-05, MI-06, MI-09, MI-11, MI-13, MI-14, MI-21, MI-23, MI-28
Bisulfite adduct of aldehyde	C(O)S(=[OX1])([O])(=[OX1])	GC376
Urea carbonyl	[NX3][CX3](=[OX1])([NX3,nX3])	Carmofur
Bis(dialkylaminethiocarbonyl)disulfide	[CX3](=[SX1])SS[CX3](=[SX1])	Disulfiram
Carbamoylsulfanyl	[NX3,nX3][C,c](=[OX1])([SX2,sx2])	Tideglusib
Disulfide	[SX2][SX2]	PX-12
Hydroxymethyl ketone	[CX3H0](=[OX1])[CH2][OH]	PF-00835231
Alkoxyethyl ketone	[CX3H0](=[OX1])[CH2][OX2H0]	2683066-41-1, 2683066-42-2, 2683066-47-7
Acyloxyethyl ketone	[CX3H0](=[OX1])[CH2][OX2H0][CX3H0](=O)	2683066-41-1, 2683066-42-2, 2683066-47-7
Fluoro, Chloro-methyl ketone	[CX3H0](=[OX1])[CH2][Cl,F]	Z-AVLD-FMK
Ebselen related	[Se]n(c=O)	Ebselen

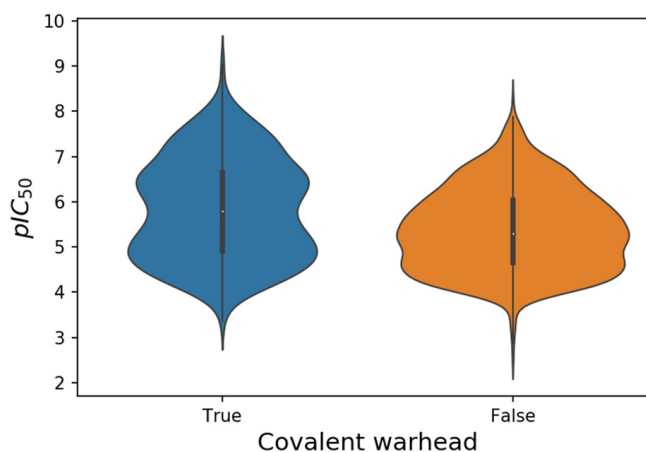
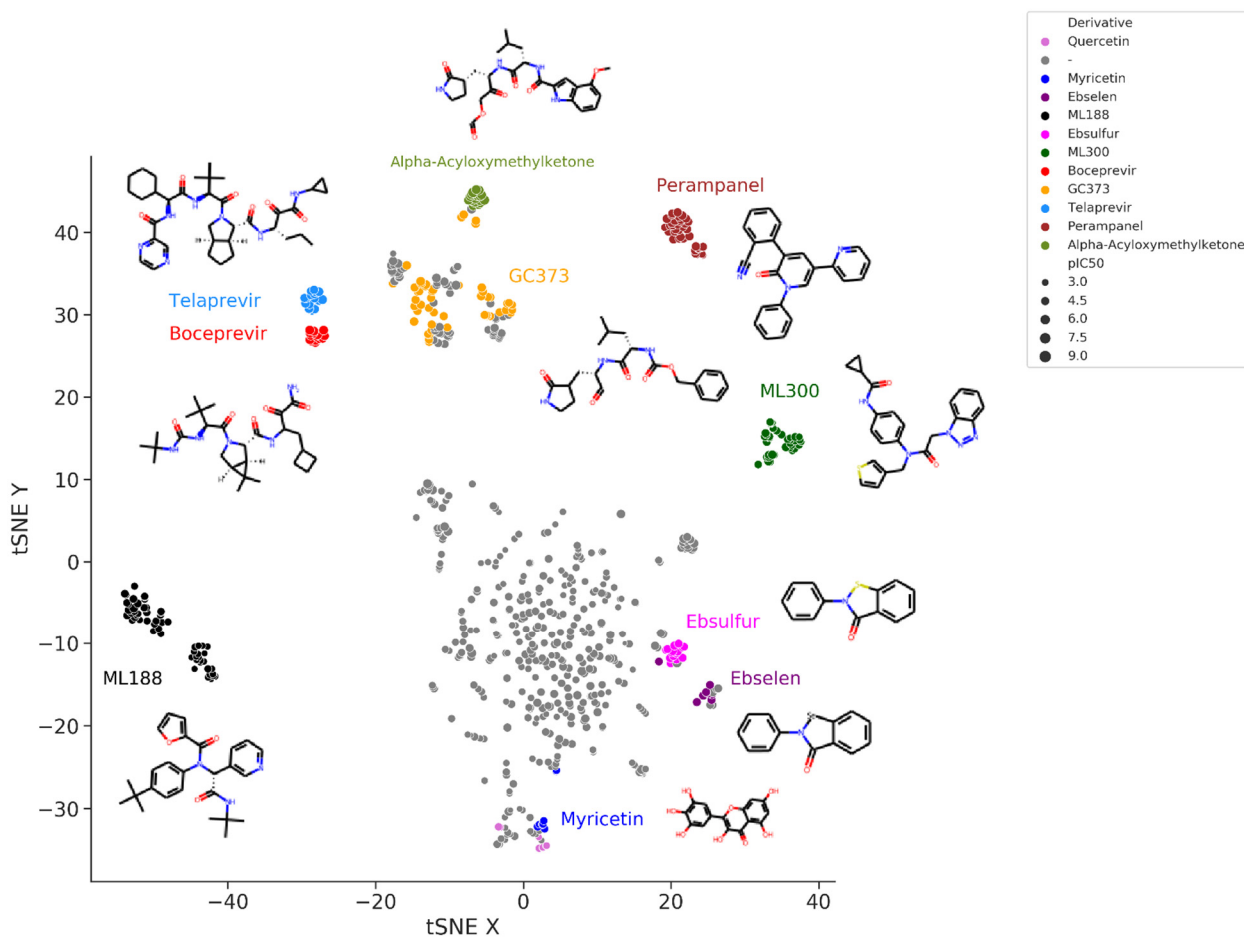
**Figure 2.** Violin plots of the pIC<sub>50</sub> values from 552 putative covalent and 1213 non-covalent SARS-CoV-2 M-pro inhibitors.

Figure 3 shows the t-Distributed Stochastic Neighbor Embedding (t-SNE) visualization of the chemical space of the set of SARS-CoV-2 M-pro inhibitors extracted from the bibliography. In this representation, more similar compounds are closer together. Peptidomimetic compounds, such as alpha-acyloxymethylketones, telaprevir, boceprevir, GC373 and their derivatives, which mimic natural peptide substrates, are closer together at the top left of the figure. Other clusters of compounds represent derivative compounds that have been synthesized from a lead compound to increase its bioactivity. Thus, derivatives from perampanel, ML300, ML188, ebsulfur, ebselen and myricetin form well-defined clusters. Perampanel derivatives are an example of a very successful increase in activity. Perampanel was first predicted as a SARS-CoV-2 M-pro inhibitor by consensus docking [2]. This prediction was confirmed by Jorgensen and coworkers, although perampanel showed only an approximate  $IC_{50}$  of 100–250  $\mu M$  [43]. The same authors also optimized this compound and synthesized several derivative compounds [44–46]. Some of these perampanel derivatives have  $IC_{50}$  values in the low nanomolar range and are some of the most potent non-covalent SARS-CoV-2 M-pro inhibitors found to date.



**Figure 3.** t-Distributed Stochastic Neighbor Embedding (t-SNE) visualization of the chemical space of a set of SARS-CoV-2 M-pro inhibitors extracted from the bibliography. Embedding is based on the 2048-bit Morgan fingerprint. Markers are colored according to several manually attributed chemotypes.

ML300 and ML188 are non-covalent inhibitors that were developed against the M-pro from SARS-CoV-1 [47,48]. Both compounds have been used to obtain more potent SARS-CoV-2 M-pro inhibitors that can inhibit SARS-CoV-2 replication in infected cells [49,50]. Boceprevir and telaprevir are approved protease inhibitors for treating hepatitis caused by the hepatitis C virus. Both compounds have been identified several times as covalent

inhibitors of the SARS-CoV-2 M-pro [43,51–58]. New bicycloproline derivatives have been designed and synthesized from them both [59]. All compounds inhibited SARS-CoV-2 M-pro in vitro, with  $IC_{50}$  values ranging from 7.6 to 748.5 nM [59]. In addition, two of them, MI-09 and MI-30, showed excellent antiviral activity in a cell-based assay and significantly reduced lung viral loads and lesions in a transgenic mouse model of SARS-CoV-2 infection [59]. GC376 is a covalent M-pro inhibitor that was developed as an inhibitor of the main protease of the feline coronavirus FCoV [60] that also showed activity against the M-pro from MERS and SARS-CoV viruses [61]. Its  $IC_{50}$  activity against SARS-CoV-2 M-pro ranges between 0.026 and 0.89  $\mu$ M [51,52,61–67]. GC376 is a prodrug, and its bisulphite adduct is converted to an aldehyde to form GC373. This aldehyde forms a covalent interaction with the catalytic Cys145 of the SARS-CoV-2 M-pro [61]. Several GC373 and GC376 derivative compounds have been designed and assayed [63,68,69]. Some of them, such as UAWJ248 [70], are more potent than GC376. A group of peptidomimetic compounds with an alpha-acyloxymethyl ketone warhead designed to form an irreversible covalent bond with Cys145 showed  $IC_{50}$  values against the SARS-CoV-2 M-pro in the nM range [71]. They also inhibited SARS-CoV-2 replication and presented low cytotoxicity and good stability [71]. Ebselen is a covalent inhibitor of the SARS-CoV-2 M-pro, although its specificity has been questioned [72,73]. Several derivative compounds of ebselen and its sulfur derivative ebsulfur have been analyzed [74,75]. Some of the derivative compounds displayed more potent M-pro inhibition than ebselen and ebsulfur [74,75]. However, the promiscuous behavior of ebselen and ebsulfur and their lack of cellular antiviral activity [74,75] may also be applied to their derivatives. Myricetin is a flavonoid that acts as a non-peptidomimetic and covalent inhibitor of SARS-CoV-2 [76,77]. Its covalent behavior was unexpected and caused by the pyrogallol moiety that formed a covalent bond with Cys145 [76]. Myricetin and its derivatives inhibit SARS-CoV-2 M-pro and SARS-CoV-2 replication in cells [76–79], and form a cluster at the bottom of Figure 3, near quercetin and other flavonoids.

### 2.1. Activity Assays for Identifying SARS-CoV-2 M-Pro Inhibitors

Several methods have been developed or adapted for quantifying the potency of the SARS-CoV-2 M-pro inhibitors [73,80–89]. These methods demonstrate the mechanism of action of antiviral drugs and do not require cells infected with SARS-CoV-2 or a laboratory with biosafety level 3 containment facilities. When combined with high-throughput sample processing and analysis, hundreds or thousands of compounds can be screened. These methods use a marked substrate, usually a peptide derivative, and when the M-pro is present, the substrate is cut, which induces the emission of a signal, usually fluorescence. In the presence of an M-pro inhibitor, signal intensity is reduced, and the potency of the inhibitor can be quantified. Some methods consist of an in vitro screen and use a purified M-pro protein, but they do not account for cell permeability, metabolism or cytotoxicity and cannot be used to accurately predict the cellular activity of M-pro inhibitors [73,83]. The M-pro protein can be expressed by transforming a bacterium with a plasmid encoding the SARS-CoV-2 M-pro. For purification purposes, an M-pro modified with the addition of specific residues, known as a tag, to the N- or C-terminus of the protein can be used. However, the tag may interfere with the binding of M-pro to its ligands [90]. M-pro requires a native N-terminus to form the active dimer [70,91], so a C-terminal His-tag has been used. However, this C-terminal His-tag can lower the binding affinity of a given ligand [90]. To overcome the limitations of the in vitro screens, cell-based assays have been developed [73,80,83,84,87,88]. In these assays, the cells express the M-pro and the reporter used and can differentiate cytotoxicity from true M-pro inhibition [83]. However, these assays often require a biosafety level 2 laboratory. To complement the activity assays, a thermal shift binding assay can be performed. This assay is based on the thermal stabilization of a protein when it binds to a protein. A  $\Delta T_m$  shift of up to 18 °C has been observed for some SARS-CoV-2 inhibitors [51,70,73,92,93]. However, the thermal shift

assay might not be suitable for analyzing non-covalent M-pro inhibitors [90]. For covalent inhibitors, the binding can be confirmed by native mass spectrometry.

In all assays for identifying SARS-CoV-2 M-pro inhibitors, negative and positive controls are needed. As a positive control, a known SARS-CoV-2 M-pro inhibitor is used. Some of the inhibitors most commonly used as positive controls are GC376, boceprevir, ebselen, disulfiram and telaprevir. After the inhibition of the SARS-CoV-2 M-pro has been detected, a dose-response assay can be used to calculate the  $IC_{50}$  or its derivative  $pIC_{50}$ . Lower values of  $IC_{50}$  and higher values of  $pIC_{50}$  represent more potent inhibitors. Comparisons between  $IC_{50}$  values obtained with different methods and by different laboratories must be made with great care. Furthermore, irreversible covalent M-pro inhibitors cannot be unambiguously ranked for potency using  $IC_{50}$  values [94]. To show the differences in the  $pIC_{50}$  estimations for the same compound, we identified the compounds with the highest number of  $pIC_{50}$  values from our dataset of SARS-CoV-2 M-pro inhibitors. Figure 4 shows the variation in the  $pIC_{50}$  values of the five most evaluated compounds, GC376, boceprevir, ebselen, disulfiram and telaprevir. These compounds are usually used as positive controls, and multiple  $pIC_{50}$  values for each compound have been calculated. The variation in the  $pIC_{50}$  values for three of these five compounds can be higher than two  $pIC_{50}$  units. This means that the estimations of the  $IC_{50}$  values of a compound could differ by a factor of 100 between two different laboratories or methods.

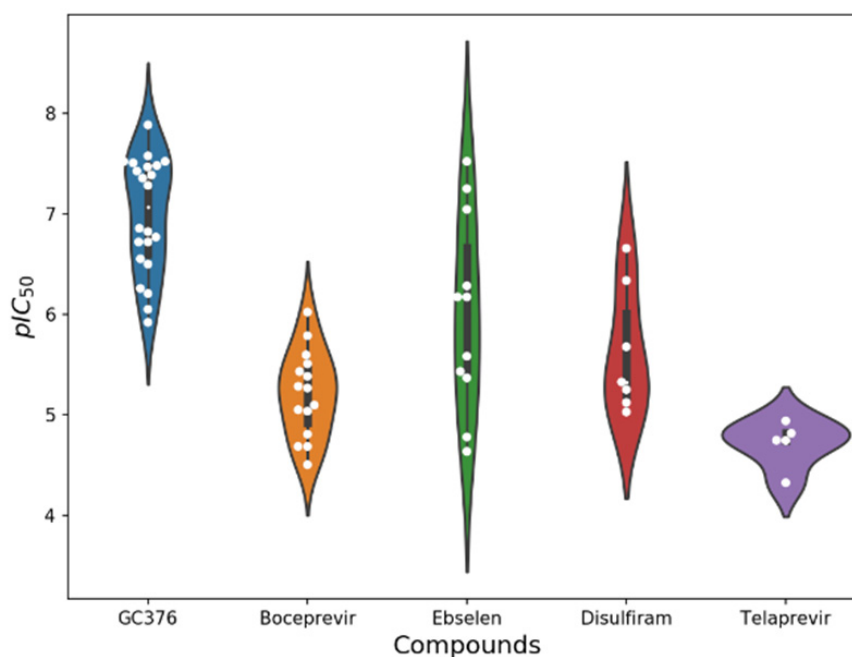


**Figure 4.** Comparison of multiple  $pIC_{50}$  values calculated by different laboratories. The  $pIC_{50}$  values of the five most evaluated compounds, GC376, boceprevir, ebselen, disulfiram and telaprevir, are shown as white points to highlight that different laboratories and methods can estimate different  $pIC_{50}$  values.

The inhibitory activity achieved in enzymatic assays is sensitive to the method and conditions used [73,95]. Compounds such as indinavir, lopinavir, nelfinavir, saquinavir, and tipranavir have shown no M-pro inhibitory activity at some of the concentrations analyzed [54,55,62,96]. Other compounds, such as candesartan, chloroquine, dipyridamole, montelukast and oxytetracycline, did not inhibit M-pro in four different assays tested [73]. The presence of DTT has been reported to affect the inhibitory activity of M-pro covalent inhibitors, as it maintains M-pro in a reduced state and eliminates non-specific thiol-reactive compounds [51,91]. Thus, if the inhibitory effect of an M-pro inhibitor is eliminated or greatly reduced by the presence of DTT, then the inhibition is non-specific. Therefore, the enzymatic inhibition potency of cysteine protease inhibitors measured in the absence of

DTT should not be used to predict cellular antiviral activity [72]. Some of the SARS-CoV-2 M-pro inhibitors whose inhibitory activity is eliminated or reduced by the presence of DTT are carmofur, disulfiram, ebselen, tideglusib, shikonin, PX-12 [72,73,97], and zinc pyrithione [77]. The results of a thermal shift-binding assay in the presence of DTT showed that some of these compounds (i.e., disulfiram, ebselen, tideglusib, shikonin and PX-12) did not bind to SARS-CoV-2 M-pro [72]. This means that these compounds are promiscuous cysteine inhibitors that are not specific for M-pro [72,73]. Figure 5 shows the effect of 1mM of DTT on the M-pro inhibition in a group of 246 SARS-CoV-2 M-pro inhibitors [77]. A total of 156 of these compounds showed a relative reduction in SARS-CoV-2 M-pro inhibition of more than 30% and can be considered as “DTT sensitive” [77].

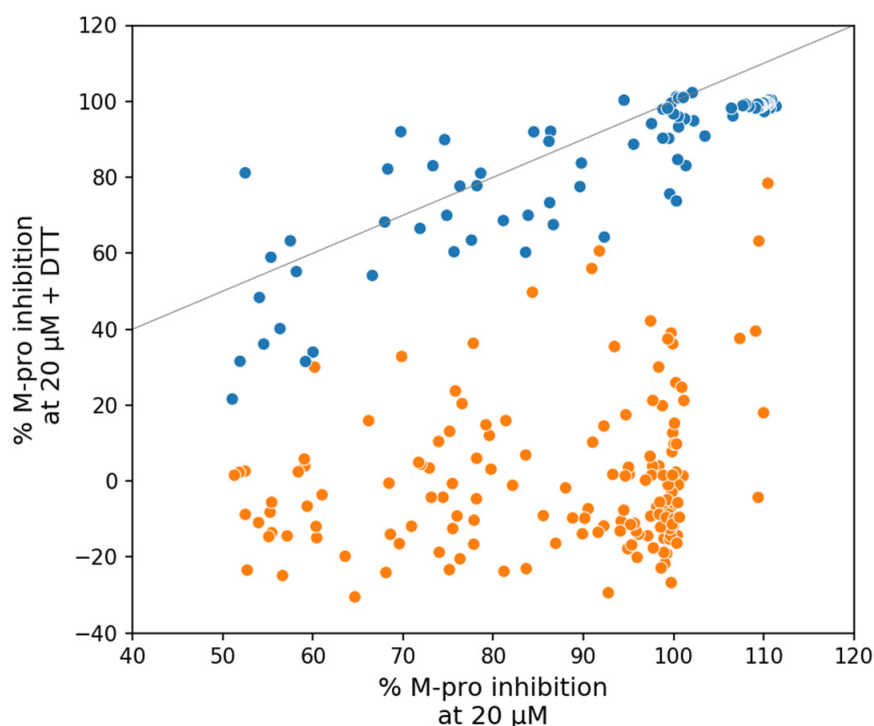


**Figure 5.** Effect of 1mM of DTT on M-pro inhibition in a group of 246 SARS-CoV-2 M-pro inhibitors [77]. A gray line represents the points where the presence of DTT does not affect the % of inhibition. Compounds far below the gray line are DTT-sensitive inhibitors and are colored orange. Compounds near the gray line are DTT insensitive inhibitors and are colored blue. The  $R^2$  value of the insensitive compounds is 0.75 ( $p = 1.1 \times 10^{-27}$ ).

## 2.2. Activity Assays for Identifying Molecules That Inhibit SARS-CoV-2 Replication

In addition to testing the inhibition of SARS-CoV-2 M-pro in vitro or in a cell-based assay, the ability of a compound to inhibit the SARS-CoV-2 replication also needs to be tested. An antiviral assay, using cells infected with SARS-CoV-2, is the gold standard assay, although it requires a biosafety level 3 laboratory. The Vero E6 cell line is one of the most common cell lines used for this analysis, but other cell lines have also been used. However, it has been reported that Vero cells express high levels of some efflux transporters, which may mask the true activity of some compounds [93]. A dose-response assay can be used to calculate a half maximal effective concentration ( $EC_{50}$ ) value, defined as the concentration of the compound that reduces the viral-induced cytopathic effect by 50% (with respect to the virus control). However, the cytotoxicity of the compounds needs to be estimated to discount that the observed effect is not due to the toxicity of the compounds. For this purpose, the half-maximal cytotoxic concentration ( $CC_{50}$ ) is usually used. Not all the compounds that inhibit the SARS-CoV-2 M-pro in vitro can inhibit the SARS-CoV-2 replication. For example, carmofur, disulfiram, ebselen, PX-2, shikonin and tideglusib



cannot inhibit SARS-CoV-2 replication in cell cultures [64,72,73]. It has been suggested that the possible antiviral activity of lopinavir and nelfinavir is due to their cytotoxicity [83,98]. The antiviral activity of other compounds against SARS-CoV-2, measured as an  $EC_{50}$  value, is slightly more than 10 times their M-pro inhibitory activity, measured as an  $IC_{50}$  value [54]. One possible explanation why compounds with high inhibitory activity in an in vitro M-pro assay show little or no activity in a cell assay is their low lipophilicity and the resulting poor cell membrane permeability. Figure 6 compares the  $pIC_{50}$  values of some SARS-CoV-2 M-pro inhibitors with their anti SARS-CoV-2 activities, measured as  $pEC_{50}$  values. To avoid comparisons between values from different laboratories, data from five articles [49,59,69,99,100] that calculate the  $pIC_{50}$  and  $pEC_{50}$  for a set of compounds are shown independently. In all but one case, the  $pEC_{50}$  values are lower than the  $pIC_{50}$  values, showing that the potency of a compound to inhibit SARS-CoV-2 replication in cells cannot always be inferred from the potency to inhibit the M-pro determined in vitro.

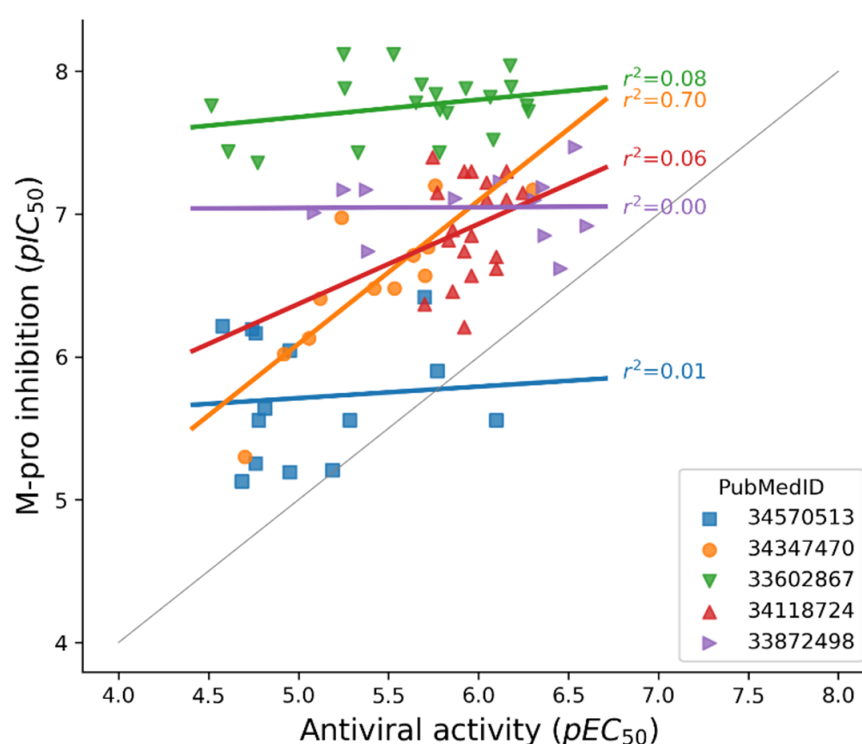


**Figure 6.** Comparison between the  $pIC_{50}$  values of some SARS-CoV-2 M-pro inhibitors and their antiviral activities, measured as  $pEC_{50}$  values. To avoid comparisons between values from different laboratories, data from five articles that calculate the  $pIC_{50}$  and  $pEC_{50}$  for a set of compounds are shown independently. The PubMedID of the articles is indicated. A gray line represents the diagonal where  $pIC_{50}$  and  $pEC_{50}$  values are equal.

### 2.3. Most Potent Covalent and Non-Covalent Inhibitors of SARS-CoV-2 M-Pro

Figure 7 and Table 3 show the 15 most potent non-covalent inhibitors of the SARS-CoV-2 M-pro. Only M-pro inhibitors that have  $pIC_{50}$  values and can inhibit SARS-CoV-2 replication in a cellular antiviral assay were included. The compound with the CAS number 339096-59-2, also named compound M3 [101], was obtained from the optimization of a previous SARS-CoV-2 M-pro inhibitor, named compound 13 [102]. Compound 339096-59-2 inhibited the SARS-CoV-2 M-pro in vitro with an  $IC_{50}$  of 13 nM and displayed anti-SARS-CoV-2 activity in Vero-E6 cells infected with SARS-CoV-2 [101]. The  $EC_{50}$  value was 16 nM [101]. This compound also inhibited in vitro human TMPRSS2 and furin enzymes, which are required for viral entry [101]. Compounds with the CAS number 2603242-35-7, 2603242-41-5, 2679814-93-6, 2679814-92-5, 2679814-91-4, 2679814-96-9, 2603242-04-0 are perampanel derivatives that can inhibit the SARS-CoV-2 M-pro in vitro, with  $IC_{50}$  values

between 0.128 and 0.018  $\mu\text{M}$  [44,46]. The most potent compounds in this set, 2603242-35-7 and 2603242-41-5, showed antiviral activity in a viral plaque assay but lacked antiviral activity in a 3-(4,5-dimethylthiazol-2-yl)-2,5-diphenyltetrazolium bromide (MTT) assay [44] (Table 3). In addition, both compounds showed the highest cytotoxicity [44]. More promising are the results of the other perampanel derivatives. In particular, 2679814-93-6 showed lower values of  $\text{EC}_{50}$  and negligible cytotoxicity in Vero E6 cells [44]. Compounds 2694063-46-0, CCF0058981, 2694063-44-8 and 2694063-65-3 are derived from ML300 with  $\text{IC}_{50}$  values against SARS-CoV-2 M-pro of 0.063, 0.068, 0.106 and 0.171  $\mu\text{M}$ , respectively [49]. CCF0058981 showed the highest anti-SARS-CoV-2 activity in infected Vero E6 cells, with an  $\text{EC}_{50}$  of 497 nM, and low cytotoxicity ( $\text{CC}_{50} > 50 \mu\text{M}$ ) [49]. The compound with the CAS number 81418-42-0 is a juglone derivative that exhibited an  $\text{IC}_{50}$  value of 72 nM against the SARS-CoV-2 M-pro and that effectively suppressed the replication of SARS-CoV-2 in Vero E6 cells [103]. Compound 392732-12-6 (MCULE-7013373725-0) is a SARS-CoV-2 M-pro inhibitor, with an  $\text{IC}_{50}$  value of 0.11  $\mu\text{M}$  that also showed significant inhibition activity against SARS-CoV-2 replication ( $\text{EC}_{50} = 0.11 \mu\text{M}$ ) [102]. Interestingly, this compound also inhibited the SARS-CoV-2 papain protease (PL-pro) and human furin protease [102]. The dual activity against the viral and host proteases and dual activity against SARS-CoV-2 M-pro and PL-pro are very interesting. However, more studies about the cytotoxicity of this compound are needed [102]. Its selectivity index (i.e., the ratio between the antiviral activity and cytotoxicity) has room for improvement [102]. PET-UNK-29afea89-2 is a 3-aminopyridine compound from the COVID Moonshot project submitted in October 2020. It showed a high SARS-CoV-2 inhibition and anti-SARS-CoV-2 activity, with  $\text{IC}_{50}$  and  $\text{EC}_{50}$  values of 0.129 and 0.244  $\mu\text{M}$ , respectively [40]. However, it was revealed to be a metabolically unstable compound [40]. The attempts to improve the stability of the compound slightly decreased compound potency but significantly increased metabolic stability and oral bioavailability [40].

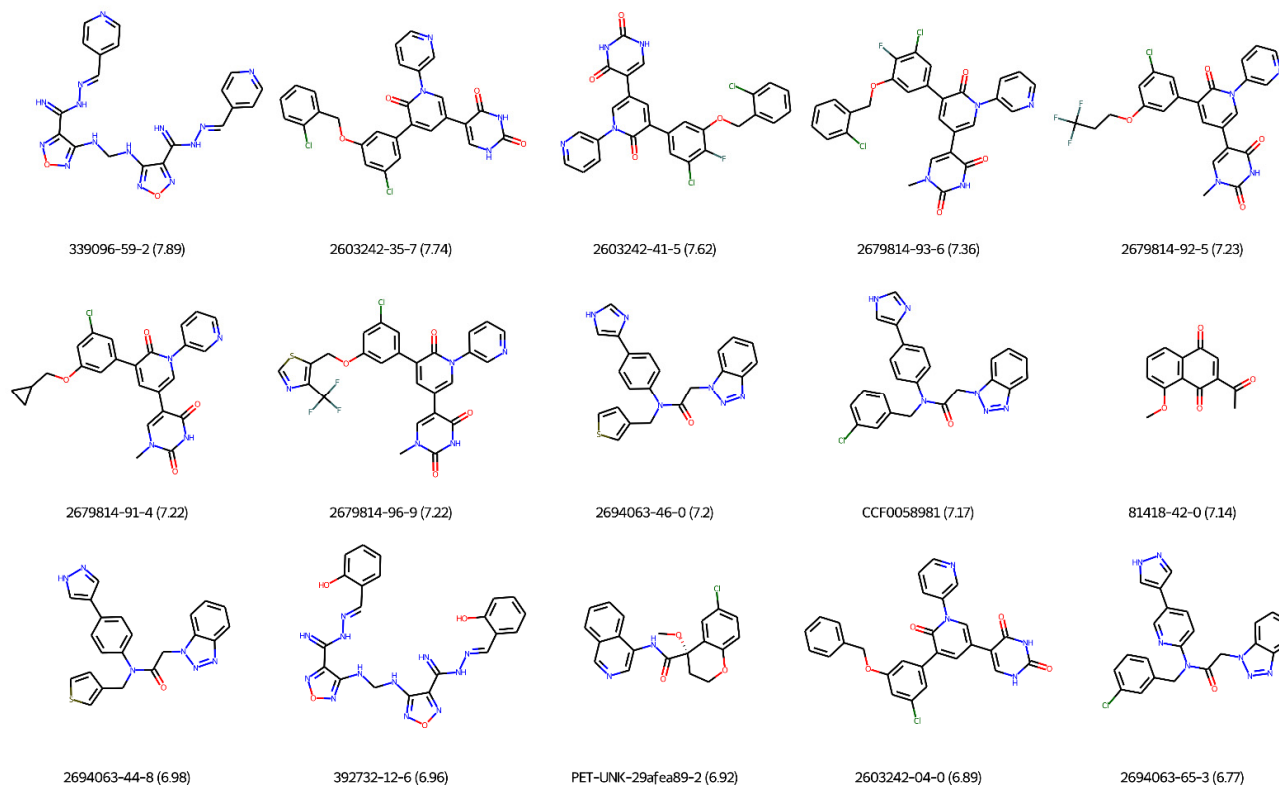


**Figure 7.** The 15 most potent non-covalent inhibitors of the SARS-CoV-2 M-pro. Only M-pro inhibitors with  $\text{pIC}_{50}$  values that can inhibit SARS-CoV-2 replication in a cellular antiviral assay are shown.  $\text{pIC}_{50}$  values are shown in parentheses.

**Table 3.** Data from the 15 most potent non-covalent inhibitors of the SARS-CoV-2 M-pro.

Compound	IC <sub>50</sub> μM (pIC <sub>50</sub> )	EC <sub>50</sub> μM	CC <sub>50</sub> μM	Reference
339096-59-2 (M3)	0.013 (7.89)	0.016 <sup>a</sup>	Higher than the EC <sub>50</sub> by 2.3-fold	[101]
2603242-35-7 (21)	0.018 (7.74)	11.30 <sup>a,b</sup>	1.7 <sup>a</sup>	[44]
2603242-41-5 (23; 18)	0.024 (7.62)	0.84 <sup>a,b</sup>	1.15 <sup>a</sup>	[44,46]
2679814-93-6 (19)	0.044 (7.36)	0.08 <sup>a</sup>	>32.5 <sup>a</sup>	[46]
2679814-92-5 (17)	0.059 (7.23)	0.82 <sup>a</sup>	>100 <sup>a</sup>	[46]
2679814-91-4 (16)	0.061 (7.22)	1.20 <sup>a</sup>	82 <sup>a</sup>	[46]
2679814-96-9 (21)	0.061 (7.22)	1.08 <sup>a</sup>	>100 <sup>a</sup>	[46]
2694063-46-0 (21)	0.063 (7.20)	1.74 <sup>a</sup>	-	[49]
CCF0058981 (41)	0.068 (7.17)	0.50 <sup>a</sup>	>50 <sup>a</sup>	[49]
81418-42-0 (15)	0.072 (7.14)	4.55 <sup>a</sup>	viability <sup>a</sup> >90% at conc. ≤ 20 μM	[103]
2694063-44-8 (19)	0.106 (6.98)	5.76 <sup>a</sup>	-	[49]
392732-12-6 (13)	0.11 (6.96)	0.11 <sup>a</sup>	0.41 <sup>c</sup>	[102]
PET-UNK-29afea89-2	0.129 (6.92)	0.244 <sup>d</sup>	lack of toxicity <sup>d</sup>	[40]
2603242-04-0 (14)	0.128 (6.89)	3.20 <sup>a</sup>	12.3 <sup>a</sup>	[44]
2694063-65-3 (40)	0.171 (6.77)	1.91 <sup>a</sup>	-	[49]

<sup>a</sup> In Vero E6 cells. <sup>b</sup> Lacked antiviral activity in an MTT assay. <sup>c</sup> In mammalian cells. <sup>d</sup> In Calu-3 cell line.

Some of the covalent inhibitors of the SARS-CoV-2 M-pro are more potent than the non-covalent inhibitors. Table 4 and Figure 8 show the 15 most potent covalent inhibitors of the SARS-CoV-2 M-pro. Only M-pro inhibitors that have pIC<sub>50</sub> values and can inhibit SARS-CoV-2 replication in a cellular antiviral assay were included. Z-AVLD-FMK is a peptidomimetic fluoromethylketone (FMK) inhibitor that was improved from a caspase inhibitor to mimic the natural substrates of the SARS-CoV-2 M-pro [97]. It has the highest inhibitory potency of all SARS-CoV-2 M-pro inhibitors, with an IC<sub>50</sub> value of 0.9 nM [97]. It also inhibited the SARS-CoV-2 replication in Vero E6 cells, with an EC<sub>50</sub> value of 66 μM [97]. Although Z-AVLD-FMK showed no toxicity at the concentrations assayed, FMKs may present host cell toxicity [97]. Z-AVLD-FMK could be used as a starting point for developing effective antiviral drugs against SARS-CoV-2 [97]. Compounds 2683066-42-2, 2683066-41-1 and 2683066-47-7 are peptidomimetic with an alpha-acyloxymethylketone warhead and a six-membered lactam glutamine mimic [71]. They are potent SARS-CoV-2 M-pro inhibitors with IC<sub>50</sub> values of 1, 6.4 and 14 nM, respectively [71]. They inhibited SARS-CoV-2 replication in Vero E6 cells and showed low cytotoxicity and good plasma and glutathione stability [71]. Compound 2683066-42-2 also displayed selectivity for SARS-CoV-2 M-pro over several cathepsins [71,93]. More advanced compounds based on alpha-acyloxymethylketone should improve metabolic stability [71]. PF-00835231 is a peptidomimetic compound with a hydroxymethylketone warhead that was a development candidate for SARS-CoV-1, but the end of the SARS-CoV-1 outbreak suspended its development [104]. It is one of the most potent SARS-CoV-2 M-pro inhibitors with an IC<sub>50</sub> value between 5.8 and 8 nM [104–106] and shows high selectivity over human proteases [93]. It exhibited potent activity against SARS-CoV-2 and other coronaviruses as a single agent [93,104]. Furthermore, PF-00835231 has synergistic activity in combination with remdesivir [93]. Pfizer has started a clinical trial of PF-07304814 (also known as lufotrelvir), a prodrug that is metabolized to PF-00835231 [93]. However, PF-07304814 must be administered by intravenous infusion, and other orally active candidates, such as PF-07321332, are better for clinical development [38]. PF-07321332 has recently been described as a SARS-CoV-2 M-pro inhibitor with in vitro pan-human coronavirus antiviral activity, excellent off-target selectivity and in vivo safety profiles [107]. It forms a reversible covalent bond with the M-pro Cys145 through a nitrile substituent [107]. Furthermore, it

has demonstrated oral activity in a mouse-adapted SARS-CoV-2 model and has achieved oral plasma concentrations exceeding the in vitro antiviral cell potency in a phase I clinical trial in healthy human participants [107]. Currently, PF-07321332 is in phase 3 trials, and it could be the first approved M-pro inhibitor to be used to treat SARS-CoV-2. MI-21, MI-23, MI-28, MI-13, MI-14, MI-05, MI-11, MI-06 and MI-09 are derivatives of boceprevir or telaprevir with  $IC_{50}$  values against the SARS-CoV-2 M-pro ranging between 7.6 and 15.2 nM [59] (Table 4). All of these compounds are aldehyde-based inhibitors and showed anti-SARS-CoV-2 activity in Vero E6 cells with  $EC_{50}$  values ranging from 0.66 to 5.63  $\mu$ M [59]. MI-30 showed an even better  $EC_{50}$  value of 0.54 nM, although its  $IC_{50}$  value (17.2 nM) is slightly higher than the previously described boceprevir or telaprevir derivatives [59]. The two compounds that showed the best anti-SARS-CoV-2 activity, MI-09 and MI-30, also improved SARS-CoV-2 induced lung lesions in a transgenic mouse model of SARS-CoV-2 infection and displayed good pharmacokinetic properties in rats [59]. UAWJ248 is a GC376 analog with an alpha-ketoamide warhead that binds irreversibly to the Cys145 from SARS-CoV-2 M-pro [70]. This compound was designed on the basis of the x-ray crystal structure of SARS-CoV-2 Mpro with GC-376 (with PDB code 6WTT), to satisfy the side-chain preferences of S1', S2, S3, and S4 M-pro pockets [70]. UAWJ248 inhibited the SARS-CoV-2 M-pro with an  $IC_{50}$  value of 12 nM [108]. However, its anti-SARS-CoV-2 potency was lower, showing an  $EC_{50}$  of 20.49  $\mu$ M against infected Vero E6 cells (Table 4) [70].

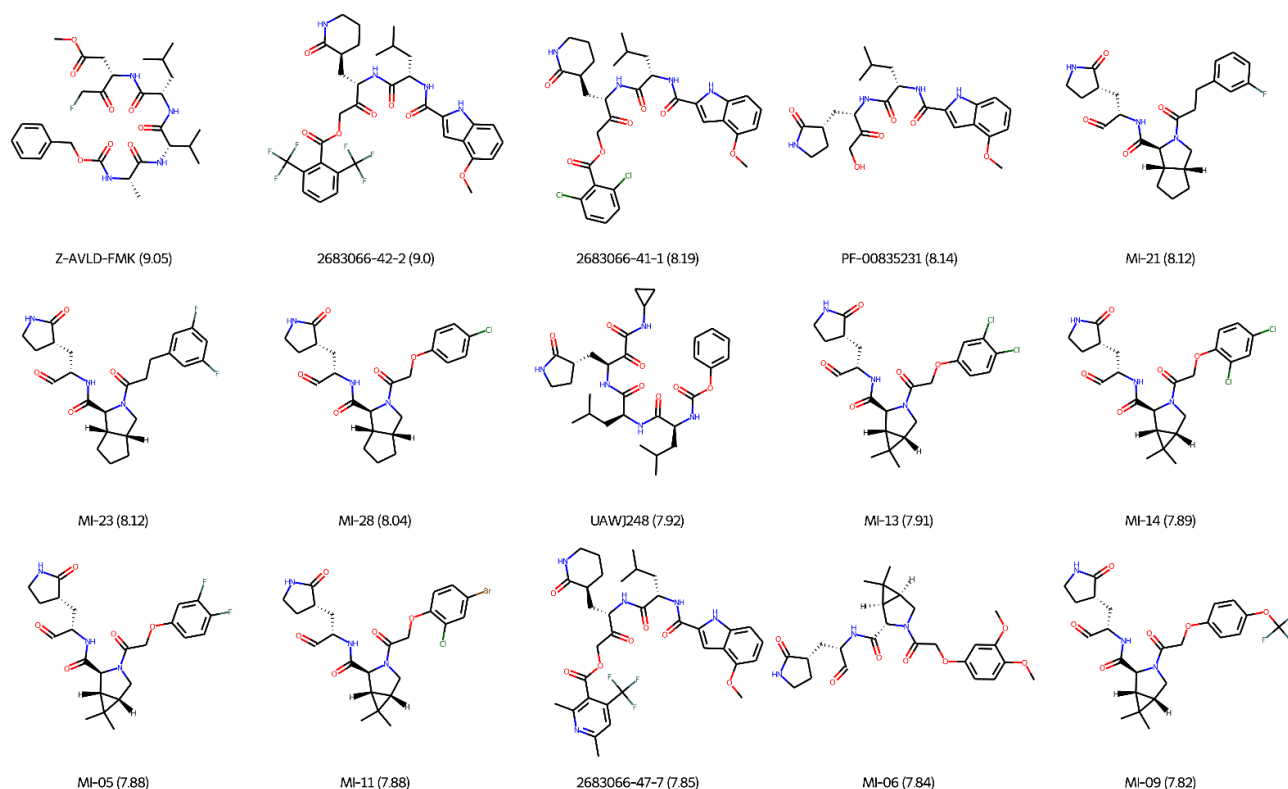


**Figure 8.** The 15 most potent covalent inhibitors of the SARS-CoV-2 M-pro. Only M-pro inhibitors with  $pIC_{50}$  values that can inhibit the SARS-CoV-2 replication in a cellular antiviral assay are shown.  $pIC_{50}$  values are shown in parentheses.

**Table 4.** Data from the 15 most potent covalent inhibitors of the SARS-CoV-2 M-pro.

Compound	IC <sub>50</sub> μM (pIC <sub>50</sub> )	EC <sub>50</sub> μM	CC <sub>50</sub> μM	Reference
Z-AVLD-FMK	0.0009 (9.05)	66.0 <sup>a</sup>	-	[97]
2683066-42-2 (15h)	0.001 (9.0)	0.16 <sup>a</sup>	>200	[71]
2683066-41-1 (15g)	0.0064 (8.19)	0.52 <sup>a</sup>	>200	[71]
PF-00835231 (4)	0.0057–0.008 0.0072 <sup>b</sup> (8.14)	88.9 <sup>a</sup>	>100 <sup>a</sup>	[93,104–106]
MI-21	0.0076 (8.12)	2.97 <sup>a</sup>	>500 <sup>a</sup>	[59]
MI-23	0.0076 (8.12)	5.63 <sup>a</sup>	>500 <sup>a</sup>	[59]
MI-28	0.0092 (8.04)	0.67 <sup>a</sup>	>500 <sup>a</sup>	[59]
UAWJ248	0.012 (7.92)	20.49 <sup>a</sup>	>250 <sup>a</sup>	[70]
MI-13	0.0124 (7.91)	2.08	>500 <sup>a</sup>	[59]
MI-14	0.0130 (7.89)	0.66 <sup>a</sup>	>500 <sup>a</sup>	[59]
MI-05	0.0132 (7.88)	5.57 <sup>a</sup>	>500 <sup>a</sup>	[59]
MI-11	0.0133 (7.88)	1.18 <sup>a</sup>	>500 <sup>a</sup>	[59]
2683066-47-7 (15m)	0.014 (7.85)	0.47 <sup>a</sup>	>200	[71]
MI-06	0.0145 (7.84)	1.73 <sup>a</sup>	>500 <sup>a</sup>	[59]
MI-09	0.0152 (7.82)	0.86 <sup>a</sup>	>500 <sup>a</sup>	[59]

<sup>a</sup> In Vero E6 cells. <sup>b</sup> Mean value of multiple IC<sub>50</sub>.

### 3. Conclusions

Since the beginning of the COVID-19 pandemic, the scientific community has tried to find a drug to inhibit the SARS-CoV-2 life cycle. The SARS-CoV-2 M-pro enzyme has been extensively studied, and its inhibitors are promising effective drugs for fighting against SARS-CoV-2. The first attempts to discover SARS-CoV-2 M-pro inhibitors used previously developed protease inhibitors or tried to repurpose drugs from other diseases. Neither attempt was entirely effective, due to, among other things, the flexibility of the SARS-CoV-2 M-pro and the inability of protein-docking methods to predict the binding modes and potency of SARS-CoV-2 M-pro inhibitors. Several *in vitro* and *in cellulo* (using live cells) methods have been developed to measure the inhibitory potency of a compound against the SARS-CoV-2 M-pro. *In vitro* methods need to express and purify SARS-CoV-2 M-pro, so some tags are sometimes added. However, especially if they are located at the N-terminus, these tags can interfere with the binding of M-pro to its ligands. The activity values obtained by different laboratories or with different methods or conditions must be compared with great care. The presence of DTT has been reported to affect the inhibitory activity of covalent M-pro inhibitors. If the inhibitory effect of an M-pro inhibitor is eliminated or greatly reduced by the presence of DTT, the inhibition is not specific. Therefore, the potency of inhibition measured in the absence of DTT should not be used by itself. The potency of a compound to inhibit SARS-CoV-2 replication in cells cannot always be inferred from the potency to inhibit M-pro, determined *in vitro*. An antiviral assay that uses cells infected with SARS-CoV-2 provides a better estimate of the potency of a compound to inhibit virus replication. However, if it is to be ruled out that the toxicity of the compounds is responsible for the antiviral activity, the cytotoxicity of the compounds needs to be determined.

In this review, we collected 1765 SARS-CoV-2 M-pro inhibitors. This set of compounds could be useful to validate a virtual screening procedure. The search for common covalent warheads identifies putative covalent inhibitors. Although we have not yet hit the bullseye and no drug has yet been approved to inhibit M-pro, we may be close. Improving derivatives of a leading compound has proven to be a very successful strategy for finding potent SARS-CoV-2 M-pro inhibitors. Some derivative compounds designed in less than two years since the start of the COVID-19 pandemic represent an important step toward the

development of new anti-SARS-CoV-2 drugs. Currently, there are several compounds with low nanomolar IC<sub>50</sub> values against SARS-CoV-2 M-pro and high anti-SARS-CoV-2 efficacy in cell models, with values comparable to those of the FDA-approved RNA polymerase inhibitor remdesivir. We hope that a SARS-CoV-2 M-pro inhibitor will be approved soon, so we can add a new tool to fight against SARS-CoV-2 or future coronavirus pandemics.

**Supplementary Materials:** The following are available online at <https://www.mdpi.com/article/10.3390/ijms23010259/s1>.

**Author Contributions:** G.P. and S.G.-V. conceived and designed the review. P.G.-S. and J.M.-T. collected the data. G.M. and B.S.-E. prepared the figures. G.M. and S.G.-V. wrote the first draft. All authors have read and agreed to the published version of the manuscript.

**Funding:** This project has received funding from the European Union's Horizon 2020 research and innovation program under the Marie Skłodowska-Curie grant agreement No. 713679 and from the Universitat Rovira i Virgili (grant 2019PFR-URV-B2-69).

**Institutional Review Board Statement:** Not applicable.

**Informed Consent Statement:** Not applicable.

**Data Availability Statement:** All data generated and analyzed during this study are included in this published article and its supplementary information files or are available from the corresponding author on reasonable request.

**Acknowledgments:** We thank ChemAxon for kindly providing us with an academic license to use their programs.

**Conflicts of Interest:** The authors declare no conflict of interest.

## References

1. Ziebuhr, J.; Herold, J.; Siddell, S.G. Characterization of a human coronavirus (strain 229E) 3C-like proteinase activity. *J. Virol.* **1995**, *69*, 4331–4338. [[CrossRef](#)]
2. Gimeno, A.; Mestres-Truyol, J.; Ojeda-Montes, M.J.; Macip, G.; Saldivar-Espinoza, B.; Cereto-Massagué, A.; Pujadas, G.; Garcia-Vallvé, S. Prediction of Novel Inhibitors of the Main Protease (M-pro) of SARS-CoV-2 through Consensus Docking and Drug Reposition. *Int. J. Mol. Sci.* **2020**, *21*, 3793. [[CrossRef](#)] [[PubMed](#)]
3. Anand, K.; Ziebuhr, J.; Wadhwani, P.; Mesters, J.R.; Hilgenfeld, R. Coronavirus main proteinase (3CLpro) structure: Basis for design of anti-SARS drugs. *Science* **2003**, *300*, 1763–1767. [[CrossRef](#)] [[PubMed](#)]
4. Jin, Z.; Du, X.; Xu, Y.; Deng, Y.; Liu, M.; Zhao, Y.; Zhang, B.; Li, X.; Zhang, L.; Peng, C.; et al. Structure of M<sup>Pro</sup> from SARS-CoV-2 and discovery of its inhibitors. *Nature* **2020**, *582*, 289–293. [[CrossRef](#)]
5. Kneller, D.W.; Phillips, G.; O'Neill, H.M.; Jedrzejczak, R.; Stols, L.; Langan, P.; Joachimiak, A.; Coates, L.; Kovalevsky, A. Structural plasticity of SARS-CoV-2 3CL M<sup>Pro</sup> active site cavity revealed by room temperature X-ray crystallography. *Nat. Commun.* **2020**, *11*, 3202. [[CrossRef](#)]
6. El-Baba, T.J.; Lutomski, C.A.; Kantsadi, A.L.; Malla, T.R.; John, T.; Mikhailov, V.; Bolla, J.R.; Schofield, C.J.; Zitzmann, N.; Vakonakis, I.; et al. Allosteric Inhibition of the SARS-CoV-2 Main Protease: Insights from Mass Spectrometry Based Assays. *Angew. Chem. Int. Ed. Engl.* **2020**, *59*, 23544–23548. [[CrossRef](#)]
7. Günther, S.; Reinke, P.Y.A.; Fernández-García, Y.; Lieske, J.; Lane, T.J.; Ginn, H.M.; Koua, F.H.M.; Ehrt, C.; Ewert, W.; Oberthuer, D.; et al. X-ray screening identifies active site and allosteric inhibitors of SARS-CoV-2 main protease. *Science* **2021**, *372*, 642–646. [[CrossRef](#)] [[PubMed](#)]
8. Du, R.; Cooper, L.; Chen, Z.; Lee, H.; Rong, L.; Cui, Q. Discovery of chebulagic acid and punicalagin as novel allosteric inhibitors of SARS-CoV-2 3CLpro. *Antivir. Res.* **2021**, *190*, 105075. [[CrossRef](#)]
9. Eberle, R.J.; Olivier, D.S.; Amaral, M.S.; Gering, I.; Willbold, D.; Arni, R.K.; Coronado, M.A. The Repurposed Drugs Suramin and Quinacrine Cooperatively Inhibit SARS-CoV-2 3CLpro In Vitro. *Viruses* **2021**, *13*, 873. [[CrossRef](#)]
10. Nguyen, D.D.; Gao, K.; Chen, J.; Wang, R.; Wei, G.-W. Unveiling the molecular mechanism of SARS-CoV-2 main protease inhibition from 137 crystal structures using algebraic topology and deep learning. *Chem. Sci.* **2020**, *11*, 12036–12046. [[CrossRef](#)]
11. Liu, Z.; Fang, H.; Reagan, K.; Xu, X.; Mendrick, D.L.; Slikker, W.; Tong, W. In silico drug repositioning: What we need to know. *Drug Discov. Today* **2013**, *18*, 110–115. [[CrossRef](#)]
12. Chakraborti, S.; Bheemireddy, S.; Srinivasan, N. Repurposing drugs against the main protease of SARS-CoV-2: Mechanism-based insights supported by available laboratory and clinical data. *Mol. Omics* **2020**, *16*, 474–491. [[CrossRef](#)]
13. Wang, X.; Guan, Y. COVID-19 drug repurposing: A review of computational screening methods, clinical trials, and protein interaction assays. *Med. Res. Rev.* **2021**, *41*, 5–28. [[CrossRef](#)] [[PubMed](#)]

14. Gimeno, A.; Ojeda-Montes, M.; Tomás-Hernández, S.; Cereto-Massagué, A.; Beltrán-Debón, R.; Mulero, M.; Pujadas, G.; Garcia-Vallvé, S. The Light and Dark Sides of Virtual Screening: What Is There to Know? *Int. J. Mol. Sci.* **2019**, *20*, 1375. [[CrossRef](#)] [[PubMed](#)]
15. Warren, G.L.; Andrews, C.W.; Capelli, A.-M.; Clarke, B.; LaLonde, J.; Lambert, M.H.; Lindvall, M.; Nevins, N.; Semus, S.F.; Senger, S.; et al. A Critical Assessment of Docking Programs and Scoring Functions. *J. Med. Chem.* **2006**, *49*, 5912–5931. [[CrossRef](#)]
16. Pantsar, T.; Poso, A. Binding Affinity via Docking: Fact and Fiction. *Molecules* **2018**, *23*, 1899. [[CrossRef](#)] [[PubMed](#)]
17. Bzówka, M.; Mitusińska, K.; Raczynska, A.; Samol, A.; Tuszyński, J.A.; Góra, A. Structural and Evolutionary Analysis Indicate That the SARS-CoV-2 M<sup>Pro</sup> Is a Challenging Target for Small-Molecule Inhibitor Design. *Int. J. Mol. Sci.* **2020**, *21*, 3099. [[CrossRef](#)]
18. Genheden, S.; Ryde, U. The MM/PBSA and MM/GBSA methods to estimate ligand-binding affinities. *Expert Opin. Drug Discov.* **2015**, *10*, 449–461. [[CrossRef](#)]
19. Macip, G.; Garcia-Segura, P.; Mestres-Truyol, J.; Saldivar-Espinoza, B.; Ojeda-Montes, M.J.; Gimeno, A.; Cereto-Massagué, A.; Garcia-Vallvé, S.; Pujadas, G. Haste makes waste: A critical review of docking-based virtual screening in drug repurposing for SARS-CoV-2 main protease (M-pro) inhibition. *Med. Res. Rev.* **2021**. [[CrossRef](#)]
20. Zev, S.; Raz, K.; Schwartz, R.; Tarabeh, R.; Gupta, P.K.; Major, D.T. Benchmarking the Ability of Common Docking Programs to Correctly Reproduce and Score Binding Modes in SARS-CoV-2 Protease M<sup>Pro</sup>. *J. Chem. Inf. Model.* **2021**, *61*, 2957–2966. [[CrossRef](#)]
21. Dotolo, S.; Marabotti, A.; Facchiano, A.; Tagliaferri, R. A review on drug repurposing applicable to COVID-19. *Brief. Bioinform.* **2021**, *22*, 726–741. [[CrossRef](#)]
22. Bellera, C.L.; Llanos, M.; Gantner, M.E.; Rodriguez, S.; Gavernet, L.; Comini, M.; Talevi, A. Can drug repurposing strategies be the solution to the COVID-19 crisis? *Expert Opin. Drug Discov.* **2021**, *16*, 605–612. [[CrossRef](#)] [[PubMed](#)]
23. Llanos, M.A.; Gantner, M.E.; Rodriguez, S.; Alberca, L.N.; Bellera, C.L.; Talevi, A.; Gavernet, L. Strengths and Weaknesses of Docking Simulations in the SARS-CoV-2 Era: The Main Protease (M<sup>Pro</sup>) Case Study. *J. Chem. Inf. Model.* **2021**, *61*, 3758–3770. [[CrossRef](#)] [[PubMed](#)]
24. Amin, S.A.; Banerjee, S.; Gayen, S.; Jha, T. Protease targeted COVID-19 drug discovery: What we have learned from the past SARS-CoV inhibitors? *Eur. J. Med. Chem.* **2021**, *215*, 113294. [[CrossRef](#)]
25. Yang, H.; Yang, J. A review of the latest research on M<sup>Pro</sup> targeting SARS-COV inhibitors. *RSC Med. Chem.* **2021**, *12*, 1026–1036. [[CrossRef](#)]
26. Cui, W.; Yang, K.; Yang, H. Recent Progress in the Drug Development Targeting SARS-CoV-2 Main Protease as Treatment for COVID-19. *Front. Mol. Biosci.* **2020**, *7*, 616341. [[CrossRef](#)]
27. Pillaiyar, T.; Wendt, L.L.; Manickam, M.; Easwaran, M. The recent outbreaks of human coronaviruses: A medicinal chemistry perspective. *Med. Res. Rev.* **2021**, *41*, 72–135. [[CrossRef](#)]
28. Banerjee, R.; Perera, L.; Tillekeratne, L.M.V. Potential SARS-CoV-2 main protease inhibitors. *Drug Discov. Today* **2021**, *26*, 804–816. [[CrossRef](#)] [[PubMed](#)]
29. Wu, F.; Zhao, S.; Yu, B.; Chen, Y.-M.; Wang, W.; Song, Z.-G.; Hu, Y.; Tao, Z.-W.; Tian, J.-H.; Pei, Y.-Y.; et al. A new coronavirus associated with human respiratory disease in China. *Nature* **2020**, *579*, 265–269. [[CrossRef](#)]
30. Gao, K.; Wang, R.; Chen, J.; Tepe, J.J.; Huang, F.; Wei, G.-W. Perspectives on SARS-CoV-2 Main Protease Inhibitors. *J. Med. Chem.* **2021**, *64*, 16922–16955. [[CrossRef](#)]
31. Xu, J.; Xue, Y.; Zhou, R.; Shi, P.; Li, H.; Zhou, J. Drug repurposing approach to combating coronavirus: Potential drugs and drug targets. *Med. Res. Rev.* **2021**, *41*, 1375–1426. [[CrossRef](#)]
32. Cannalire, R.; Cerchia, C.; Beccari, A.R.; Di Leva, F.S.; Summa, V. Targeting SARS-CoV-2 Proteases and Polymerase for COVID-19 Treatment: State of the Art and Future Opportunities. *J. Med. Chem.* **2020**. [[CrossRef](#)]
33. Chen, C.; Yu, X.; Kuo, C.; Min, J.; Chen, S.; Ma, L.; Liu, K.; Guo, R. Overview of antiviral drug candidates targeting coronaviral 3C-like main proteases. *FEBS J.* **2021**, *288*, 5089–5121. [[CrossRef](#)]
34. Xiong, M.; Su, H.; Zhao, W.; Xie, H.; Shao, Q.; Xu, Y. What coronavirus 3C-like protease tells us: From structure, substrate selectivity, to inhibitor design. *Med. Res. Rev.* **2021**, *41*, 1965–1998. [[CrossRef](#)]
35. Mengist, H.M.; Dilnessa, T.; Jin, T. Structural Basis of Potential Inhibitors Targeting SARS-CoV-2 Main Protease. *Front. Chem.* **2021**, *9*, 622898. [[CrossRef](#)] [[PubMed](#)]
36. Citarella, A.; Scala, A.; Piperno, A.; Micale, N. SARS-CoV-2 M<sup>Pro</sup>: A Potential Target for Peptidomimetics and Small-Molecule Inhibitors. *Biomolecules* **2021**, *11*, 607. [[CrossRef](#)]
37. Chia, C.S.B.; Xu, W.; Shuyi Ng, P. A Patent Review on SARS Coronavirus Main Protease (3CL pro) Inhibitors. *ChemMedChem* **2021**. [[CrossRef](#)] [[PubMed](#)]
38. Vandyck, K.; Deval, J. Considerations for the discovery and development of 3-chymotrypsin-like cysteine protease inhibitors targeting SARS-CoV-2 infection. *Curr. Opin. Virol.* **2021**, *49*, 36–40. [[CrossRef](#)] [[PubMed](#)]
39. COVID Moonshot. Available online: <https://covid.postera.ai/covid> (accessed on 1 October 2021).
40. The COVID Moonshot Consortium; Chodera, J.; Lee, A.; London, N.; von Delft, F. Open Science Discovery of Oral Non-Covalent SARS-CoV-2 Main Protease Inhibitors. *ChemRxiv* **2021**. [[CrossRef](#)]
41. Mendez, D.; Gaulton, A.; Bento, A.P.; Chambers, J.; De Veij, M.; Félix, E.; Magariños, M.P.; Mosquera, J.F.; Mutowo, P.; Nowotka, M.; et al. ChEMBL: Towards direct deposition of bioassay data. *Nucleic Acids Res.* **2019**, *47*, D930–D940. [[CrossRef](#)]
42. Singh, J.; Petter, R.C.; Baillie, T.A.; Whitty, A. The resurgence of covalent drugs. *Nat. Rev. Drug Discov.* **2011**, *10*, 307–317. [[CrossRef](#)]

43. Ghahremanpour, M.M.; Tirado-Rives, J.; Deshmukh, M.; Ippolito, J.A.; Zhang, C.-H.; Cabeza de Vaca, I.; Liosi, M.-E.; Anderson, K.S.; Jorgensen, W.L. Identification of 14 Known Drugs as Inhibitors of the Main Protease of SARS-CoV-2. *ACS Med. Chem. Lett.* **2020**, *11*, 2526–2533. [[CrossRef](#)]
44. Zhang, C.-H.; Stone, E.A.; Deshmukh, M.; Ippolito, J.A.; Ghahremanpour, M.M.; Tirado-Rives, J.; Spasov, K.A.; Zhang, S.; Takeo, Y.; Kudalkar, S.N.; et al. Potent Noncovalent Inhibitors of the Main Protease of SARS-CoV-2 from Molecular Sculpting of the Drug Perampanel Guided by Free Energy Perturbation Calculations. *ACS Cent. Sci.* **2021**, *7*, 467–475. [[CrossRef](#)] [[PubMed](#)]
45. Deshmukh, M.G.; Ippolito, J.A.; Zhang, C.-H.; Stone, E.A.; Reilly, R.A.; Miller, S.J.; Jorgensen, W.L.; Anderson, K.S. Structure-guided design of a perampanel-derived pharmacophore targeting the SARS-CoV-2 main protease. *Structure* **2021**, *29*, 823–833.e5. [[CrossRef](#)] [[PubMed](#)]
46. Zhang, C.-H.; Spasov, K.A.; Reilly, R.A.; Hollander, K.; Stone, E.A.; Ippolito, J.A.; Liosi, M.-E.; Deshmukh, M.G.; Tirado-Rives, J.; Zhang, S.; et al. Optimization of Triarylpyridinone Inhibitors of the Main Protease of SARS-CoV-2 to Low-Nanomolar Antiviral Potency. *ACS Med. Chem. Lett.* **2021**, *12*, 1325–1332. [[CrossRef](#)] [[PubMed](#)]
47. Jacobs, J.; Grum-Tokars, V.; Zhou, Y.; Turlington, M.; Saldanha, S.A.; Chase, P.; Egger, A.; Dawson, E.S.; Baez-Santos, Y.M.; Tomar, S.; et al. Discovery, synthesis, and structure-based optimization of a series of N-(tert-butyl)-2-(N-arylamido)-2-(pyridin-3-yl) acetamides (ML188) as potent noncovalent small molecule inhibitors of the severe acute respiratory syndrome coronavirus (SARS-CoV) 3CL pro. *J. Med. Chem.* **2013**, *56*, 534–546. [[CrossRef](#)] [[PubMed](#)]
48. Turlington, M.; Chun, A.; Tomar, S.; Egger, A.; Grum-Tokars, V.; Jacobs, J.; Daniels, J.S.; Dawson, E.; Saldanha, A.; Chase, P.; et al. Discovery of N-(benzo[1,2,3]triazol-1-yl)-N-(benzyl)acetamido)phenyl) carboxamides as severe acute respiratory syndrome coronavirus (SARS-CoV) 3CLpro inhibitors: Identification of ML300 and noncovalent nanomolar inhibitors with an induced-fit binding. *Bioorg. Med. Chem. Lett.* **2013**, *23*, 6172–6177. [[CrossRef](#)] [[PubMed](#)]
49. Han, S.H.; Goins, C.M.; Arya, T.; Shin, W.-J.; Maw, J.; Hooper, A.; Sonawane, D.P.; Porter, M.R.; Bannister, B.E.; Crouch, R.D.; et al. Structure-Based Optimization of ML300-Derived, Noncovalent Inhibitors Targeting the Severe Acute Respiratory Syndrome Coronavirus 3CL Protease (SARS-CoV-2 3CL pro). *J. Med. Chem.* **2021**. [[CrossRef](#)]
50. Kitamura, N.; Sacco, M.D.; Ma, C.; Hu, Y.; Townsend, J.A.; Meng, X.; Zhang, F.; Zhang, X.; Ba, M.; Szeto, T.; et al. Expedited Approach toward the Rational Design of Noncovalent SARS-CoV-2 Main Protease Inhibitors. *J. Med. Chem.* **2021**. [[CrossRef](#)] [[PubMed](#)]
51. Ma, C.; Sacco, M.D.; Hurst, B.; Townsend, J.A.; Hu, Y.; Szeto, T.; Zhang, X.; Tarbet, B.; Marty, M.T.; Chen, Y.; et al. Boceprevir, GC-376, and calpain inhibitors II, XII inhibit SARS-CoV-2 viral replication by targeting the viral main protease. *Cell Res.* **2020**, *30*, 678–692. [[CrossRef](#)]
52. Fu, L.; Ye, F.; Feng, Y.; Yu, F.; Wang, Q.; Wu, Y.; Zhao, C.; Sun, H.; Huang, B.; Niu, P.; et al. Both Boceprevir and GC376 efficaciously inhibit SARS-CoV-2 by targeting its main protease. *Nat. Commun.* **2020**, *11*, 4417. [[CrossRef](#)]
53. Kneller, D.W.; Galanie, S.; Phillips, G.; O'Neill, H.M.; Coates, L.; Kovalevsky, A. Malleability of the SARS-CoV-2 3CL M<sup>Pro</sup> Active-Site Cavity Facilitates Binding of Clinical Antivirals. *Structure* **2020**, *28*, 1313–1320.e3. [[CrossRef](#)]
54. Pathak, N.; Chen, Y.-T.; Hsu, Y.-C.; Hsu, N.-Y.; Kuo, C.-J.; Tsai, H.P.; Kang, J.-J.; Huang, C.-H.; Chang, S.-Y.; Chang, Y.-H.; et al. Uncovering Flexible Active Site Conformations of SARS-CoV-2 3CL Proteases through Protease Pharmacophore Clusters and COVID-19 Drug Repurposing. *ACS Nano* **2021**, *15*, 857–872. [[CrossRef](#)]
55. Jan, J.-T.; Cheng, T.-J.R.; Juang, Y.-P.; Ma, H.-H.; Wu, Y.-T.; Yang, W.-B.; Cheng, C.-W.; Chen, X.; Chou, T.-H.; Shie, J.-J.; et al. Identification of existing pharmaceuticals and herbal medicines as inhibitors of SARS-CoV-2 infection. *Proc. Natl. Acad. Sci. USA* **2021**, *118*, e2021579118. [[CrossRef](#)] [[PubMed](#)]
56. Mody, V.; Ho, J.; Wills, S.; Mawri, A.; Lawson, L.; Ebert, M.C.C.J.C.; Fortin, G.M.; Rayalam, S.; Taval, S. Identification of 3-chymotrypsin like protease (3CLPro) inhibitors as potential anti-SARS-CoV-2 agents. *Commun. Biol.* **2021**, *4*, 93. [[CrossRef](#)] [[PubMed](#)]
57. Baker, J.D.; Uhrich, R.L.; Kraemer, G.C.; Love, J.E.; Kraemer, B.C. A drug repurposing screen identifies hepatitis C antivirals as inhibitors of the SARS-CoV2 main protease. *PLoS ONE* **2021**, *16*, e0245962. [[CrossRef](#)]
58. Manandhar, A.; Blass, B.E.; Colussi, D.J.; Almi, I.; Abou-Gharbia, M.; Klein, M.L.; Elokely, K.M. Targeting SARS-CoV-2 M3CLpro by HCV NS3/4a Inhibitors: In Silico Modeling and In Vitro Screening. *J. Chem. Inf. Model.* **2021**, *61*, 1020–1032. [[CrossRef](#)] [[PubMed](#)]
59. Qiao, J.; Li, Y.-S.; Zeng, R.; Liu, F.-L.; Luo, R.-H.; Huang, C.; Wang, Y.-F.; Zhang, J.; Quan, B.; Shen, C.; et al. SARS-CoV-2 M<sup>Pro</sup> inhibitors with antiviral activity in a transgenic mouse model. *Science* **2021**, *371*, 1374–1378. [[CrossRef](#)]
60. Kim, Y.; Shivanna, V.; Narayanan, S.; Prior, A.M.; Weerasekera, S.; Hua, D.H.; Kankanamalage, A.C.G.; Groutas, W.C.; Chang, K.-O. Broad-spectrum inhibitors against 3C-like proteases of feline coronaviruses and feline caliciviruses. *J. Virol.* **2015**, *89*, 4942–4950. [[CrossRef](#)]
61. Vuong, W.; Khan, M.B.; Fischer, C.; Arutyunova, E.; Lamer, T.; Shields, J.; Saffran, H.A.; McKay, R.T.; van Belkum, M.J.; Joyce, M.A.; et al. Feline coronavirus drug inhibits the main protease of SARS-CoV-2 and blocks virus replication. *Nat. Commun.* **2020**, *11*, 4282. [[CrossRef](#)]
62. Hung, H.; Ke, Y.; Huang, S.Y.; Huang, P.-N.; Kung, Y.; Chang, T.-Y.; Yen, K.; Peng, T.-T.; Chang, S.-E.; Huang, C.-T.; et al. Discovery of M Protease Inhibitors Encoded by SARS-CoV-2. *Antimicrob. Agents Chemother.* **2020**, *64*, e00872-20. [[CrossRef](#)]



63. Rathnayake, A.D.; Zheng, J.; Kim, Y.; Perera, K.D.; Mackin, S.; Meyerholz, D.K.; Kashipathy, M.M.; Battaile, K.P.; Lovell, S.; Perlman, S.; et al. 3C-like protease inhibitors block coronavirus replication in vitro and improve survival in MERS-CoV-infected mice. *Sci. Transl. Med.* **2020**, *12*, eabc5332. [[CrossRef](#)] [[PubMed](#)]
64. Gurard-Levin, Z.A.; Liu, C.; Jekle, A.; Jaisinghani, R.; Ren, S.; Vandyck, K.; Jochmans, D.; Leyssen, P.; Neyts, J.; Blatt, L.M.; et al. Evaluation of SARS-CoV-2 3C-like protease inhibitors using self-assembled monolayer desorption ionization mass spectrometry. *Antivir. Res.* **2020**, *182*, 104924. [[CrossRef](#)]
65. Wang, Y.-C.; Yang, W.-H.; Yang, C.-S.; Hou, M.-H.; Tsai, C.-L.; Chou, Y.-Z.; Hung, M.-C.; Chen, Y. Structural basis of SARS-CoV-2 main protease inhibition by a broad-spectrum anti-coronaviral drug. *Am. J. Cancer Res.* **2020**, *10*, 2535–2545.
66. Zhu, W.; Xu, M.; Chen, C.Z.; Guo, H.; Shen, M.; Hu, X.; Shinn, P.; Klumpp-Thomas, C.; Michael, S.G.; Zheng, W. Identification of SARS-CoV-2 3CL Protease Inhibitors by a Quantitative High-Throughput Screening. *ACS Pharmacol. Transl. Sci.* **2020**, *3*, 1008–1016. [[CrossRef](#)]
67. Iketani, S.; Forouhar, F.; Liu, H.; Hong, S.J.; Lin, F.-Y.; Nair, M.S.; Zask, A.; Huang, Y.; Xing, L.; Stockwell, B.R.; et al. Lead compounds for the development of SARS-CoV-2 3CL protease inhibitors. *Nat. Commun.* **2021**, *12*, 2016. [[CrossRef](#)] [[PubMed](#)]
68. Yang, K.S.; Ma, X.R.; Ma, Y.; Alugubelli, Y.R.; Scott, D.A.; Vatanserver, E.C.; Drelich, A.K.; Sankaran, B.; Geng, Z.Z.; Blankenship, L.R.; et al. A Quick Route to Multiple Highly Potent SARS-CoV-2 Main Protease Inhibitors. *ChemMedChem* **2021**, *16*, 942–948. [[CrossRef](#)]
69. Vuong, W.; Fischer, C.; Khan, M.B.; van Belkum, M.J.; Lamer, T.; Willoughby, K.D.; Lu, J.; Arutyunova, E.; Joyce, M.A.; Saffran, H.A.; et al. Improved SARS-CoV-2 M<sup>Pro</sup> inhibitors based on feline antiviral drug GC376: Structural enhancements, increased solubility, and micellar studies. *Eur. J. Med. Chem.* **2021**, *222*, 113584. [[CrossRef](#)]
70. Sacco, M.D.; Ma, C.; Lagarias, P.; Gao, A.; Townsend, J.A.; Meng, X.; Dube, P.; Zhang, X.; Hu, Y.; Kitamura, N.; et al. Structure and inhibition of the SARS-CoV-2 main protease reveal strategy for developing dual inhibitors against M<sup>Pro</sup> and cathepsin L. *Sci. Adv.* **2020**, *6*, eabe0751. [[CrossRef](#)] [[PubMed](#)]
71. Bai, B.; Belovodskiy, A.; Hena, M.; Kandadai, A.S.; Joyce, M.A.; Saffran, H.A.; Shields, J.A.; Khan, M.B.; Arutyunova, E.; Lu, J.; et al. Peptidomimetic  $\alpha$ -Acylloxymethylketone Warheads with Six-Membered Lactam P1 Glutamine Mimic: SARS-CoV-2 3CL Protease Inhibition, Coronavirus Antiviral Activity, and in Vitro Biological Stability. *J. Med. Chem.* **2021**. [[CrossRef](#)]
72. Ma, C.; Hu, Y.; Townsend, J.A.; Lagarias, P.I.; Marty, M.T.; Kolocouris, A.; Wang, J. Ebselen, Disulfiram, Carmofur, PX-12, Tideglusib, and Shikonin Are Nonspecific Promiscuous SARS-CoV-2 Main Protease Inhibitors. *ACS Pharmacol. Transl. Sci.* **2020**, *3*, 1265–1277. [[CrossRef](#)] [[PubMed](#)]
73. Ma, C.; Tan, H.; Choza, J.; Wang, Y.; Wang, J. Validation and invalidation of SARS-CoV-2 main protease inhibitors using the Flip-GFP and Protease-Glo luciferase assays. *Acta Pharm. Sin. B* **2021**. [[CrossRef](#)]
74. Sun, L.-Y.; Chen, C.; Su, J.; Li, J.-Q.; Jiang, Z.; Gao, H.; Chigan, J.-Z.; Ding, H.-H.; Zhai, L.; Yang, K.-W. Ebsulfur and Ebselen as highly potent scaffolds for the development of potential SARS-CoV-2 antivirals. *Bioorg. Chem.* **2021**, *112*, 104889. [[CrossRef](#)]
75. Ampornadani, K.; Meng, X.; Shang, W.; Jin, Z.; Rogers, M.; Zhao, Y.; Rao, Z.; Liu, Z.-J.; Yang, H.; Zhang, L.; et al. Inhibition mechanism of SARS-CoV-2 main protease by ebselen and its derivatives. *Nat. Commun.* **2021**, *12*, 3061. [[CrossRef](#)]
76. Su, H.; Yao, S.; Zhao, W.; Zhang, Y.; Liu, J.; Shao, Q.; Wang, Q.; Li, M.; Xie, H.; Shang, W.; et al. Identification of pyrogallol as a warhead in design of covalent inhibitors for the SARS-CoV-2 3CL protease. *Nat. Commun.* **2021**, *12*, 3623. [[CrossRef](#)] [[PubMed](#)]
77. Kuzikov, M.; Costanzi, E.; Reinshagen, J.; Esposito, F.; Vangeel, L.; Wolf, M.; Ellinger, B.; Claussen, C.; Geisslinger, G.; Corona, A.; et al. Identification of Inhibitors of SARS-CoV-2 3CL-Pro Enzymatic Activity Using a Small Molecule in Vitro Repurposing Screen. *ACS Pharmacol. Transl. Sci.* **2021**, *4*, 1096–1110. [[CrossRef](#)]
78. Liu, H.; Ye, F.; Sun, Q.; Liang, H.; Li, C.; Li, S.; Lu, R.; Huang, B.; Tan, W.; Lai, L. Scutellaria baicalensis extract and baicalein inhibit replication of SARS-CoV-2 and its 3C-like protease in vitro. *J. Enzyme Inhib. Med. Chem.* **2021**, *36*, 497–503. [[CrossRef](#)] [[PubMed](#)]
79. Nguyen, T.T.H.; Jung, J.-H.; Kim, M.-K.; Lim, S.; Choi, J.-M.; Chung, B.; Kim, D.-W.; Kim, D. The Inhibitory Effects of Plant Derivate Polyphenols on the Main Protease of SARS Coronavirus 2 and Their Structure–Activity Relationship. *Molecules* **2021**, *26*, 1924. [[CrossRef](#)] [[PubMed](#)]
80. Froggatt, H.M.; Heaton, B.E.; Heaton, N.S. Development of a Fluorescence-Based, High-Throughput SARS-CoV-2 3CLpro Reporter Assay. *J. Virol.* **2020**, *94*, e01265-20. [[CrossRef](#)]
81. Franko, N.; Teixeira, A.P.; Xue, S.; Charpin-El Hamri, G.; Fussenegger, M. Design of modular autoproteolytic gene switches responsive to anti-coronavirus drug candidates. *Nat. Commun.* **2021**, *12*, 6786. [[CrossRef](#)]
82. Coelho, C.; Gallo, G.; Campos, C.B.; Hardy, L.; Würtele, M. Biochemical screening for SARS-CoV-2 main protease inhibitors. *PLoS ONE* **2020**, *15*, e0240079. [[CrossRef](#)] [[PubMed](#)]
83. Rawson, J.M.O.; Duchon, A.; Nikolaitchik, O.A.; Pathak, V.K.; Hu, W.-S. Development of a Cell-Based Luciferase Complementation Assay for Identification of SARS-CoV-2 3CLpro Inhibitors. *Viruses* **2021**, *13*, 173. [[CrossRef](#)] [[PubMed](#)]
84. O'Brien, A.; Chen, D.-Y.; Hackbart, M.; Close, B.J.; O'Brien, T.E.; Saeed, M.; Baker, S.C. Detecting SARS-CoV-2 3CLpro expression and activity using a polyclonal antiserum and a luciferase-based biosensor. *Virology* **2021**, *556*, 73–78. [[CrossRef](#)] [[PubMed](#)]
85. Dražić, T.; Kühn, N.; Leuthold, M.M.; Behnam, M.A.M.; Klein, C.D. Efficiency Improvements and Discovery of New Substrates for a SARS-CoV-2 Main Protease FRET Assay. *SLAS Discov. Adv. Sci. Drug Discov.* **2021**, *26*, 1189–1199. [[CrossRef](#)]
86. Ihssen, J.; Faccio, G.; Yao, C.; Sirec, T.; Spitz, U. Fluorogenic in vitro activity assay for the main protease M<sup>Pro</sup> from SARS-CoV-2 and its adaptation to the identification of inhibitors. *STAR Protoc.* **2021**, *2*, 100793. [[CrossRef](#)]

87. Mathieu, C.; Touret, F.; Jacquemin, C.; Janin, Y.L.; Nougairède, A.; Brailly, M.; Mazelier, M.; Décimo, D.; Vasseur, V.; Hans, A.; et al. A Bioluminescent 3CLPro Activity Assay to Monitor SARS-CoV-2 Replication and Identify Inhibitors. *Viruses* **2021**, *13*, 1814. [[CrossRef](#)]
88. Dey-Rao, R.; Smith, G.R.; Timilsina, U.; Falls, Z.; Samudrala, R.; Stavrou, S.; Melendy, T. A fluorescence-based, gain-of-signal, live cell system to evaluate SARS-CoV-2 main protease inhibition. *Antiviral Res.* **2021**, *195*, 105183. [[CrossRef](#)]
89. Alalam, H.; Sigurdardóttir, S.; Bourgard, C.; Tiukova, I.; King, R.D.; Grøtli, M.; Sunnerhagen, P. A Genetic Trap in Yeast for Inhibitors of SARS-CoV-2 Main Protease. *mSystems* **2021**, *6*, e0108721. [[CrossRef](#)]
90. Li, Z.; Lin, Y.; Huang, Y.-Y.; Liu, R.; Zhan, C.-G.; Wang, X.; Luo, H.-B. Reply to Ma and Wang: Reliability of various in vitro activity assays on SARS-CoV-2 main protease inhibitors. *Proc. Natl. Acad. Sci. USA* **2021**, *118*, e2024937118. [[CrossRef](#)] [[PubMed](#)]
91. Ma, C.; Wang, J. Dipyrindamole, chloroquine, montelukast sodium, candesartan, oxytetracycline, and atazanavir are not SARS-CoV-2 main protease inhibitors. *Proc. Natl. Acad. Sci. USA* **2021**, *118*, e2024420118. [[CrossRef](#)]
92. Xia, Z.; Sacco, M.; Hu, Y.; Ma, C.; Meng, X.; Zhang, F.; Szeto, T.; Xiang, Y.; Chen, Y.; Wang, J. Rational Design of Hybrid SARS-CoV-2 Main Protease Inhibitors Guided by the Superimposed Cocrystal Structures with the Peptidomimetic Inhibitors GC-376, Telaprevir, and Boceprevir. *ACS Pharmacol. Transl. Sci.* **2021**, *4*, 1408–1421. [[CrossRef](#)]
93. Boras, B.; Jones, R.M.; Anson, B.J.; Arenson, D.; Aschenbrenner, L.; Bakowski, M.A.; Beutler, N.; Binder, J.; Chen, E.; Eng, H.; et al. Preclinical characterization of an intravenous coronavirus 3CL protease inhibitor for the potential treatment of COVID19. *Nat. Commun.* **2021**, *12*, 6055. [[CrossRef](#)] [[PubMed](#)]
94. Gossen, J.; Albani, S.; Hanke, A.; Joseph, B.P.; Bergh, C.; Kuzikov, M.; Costanzi, E.; Manelfi, C.; Storici, P.; Gribbon, P.; et al. A Blueprint for High Affinity SARS-CoV-2 M<sup>Pro</sup> Inhibitors from Activity-Based Compound Library Screening Guided by Analysis of Protein Dynamics. *ACS Pharmacol. Transl. Sci.* **2021**, *4*, 1079–1095. [[CrossRef](#)] [[PubMed](#)]
95. Behnam, M.A.M.; Klein, C.D. Inhibitor potency and assay conditions: A case study on SARS-CoV-2 main protease. *Proc. Natl. Acad. Sci. USA* **2021**, *118*, e2106095118. [[CrossRef](#)] [[PubMed](#)]
96. Mahdi, M.; Mótóyán, J.A.; Szojka, Z.I.; Golda, M.; Miczi, M.; Tózsér, J. Analysis of the efficacy of HIV protease inhibitors against SARS-CoV-2's main protease. *Virology* **2020**, *17*, 190. [[CrossRef](#)] [[PubMed](#)]
97. Milligan, J.C.; Zeisner, T.U.; Papageorgiou, G.; Joshi, D.; Soudy, C.; Ulferts, R.; Wu, M.; Lim, C.T.; Tan, K.W.; Weissmann, F.; et al. Identifying SARS-CoV-2 antiviral compounds by screening for small molecule inhibitors of Nsp5 main protease. *Biochem. J.* **2021**, *478*, 2499–2515. [[CrossRef](#)] [[PubMed](#)]
98. Hattori, S.; Higshi-Kuwata, N.; Raghavaiah, J.; Das, D.; Bulut, H.; Davis, D.A.; Takamatsu, Y.; Matsuda, K.; Takamune, N.; Kishimoto, N.; et al. GRL-0920, an Indole Chloropyridinyl Ester, Completely Blocks SARS-CoV-2 Infection. *mBio* **2020**, *11*, e01833-20. [[CrossRef](#)]
99. Huff, S.; Kummetha, I.R.; Tiwari, S.K.; Huante, M.B.; Clark, A.E.; Wang, S.; Bray, W.; Smith, D.; Carlin, A.F.; Endsley, M.; et al. Discovery and Mechanism of SARS-CoV-2 Main Protease Inhibitors. *J. Med. Chem.* **2021**. [[CrossRef](#)]
100. Dai, W.; Jochmans, D.; Xie, H.; Yang, H.; Li, J.; Su, H.; Chang, D.; Wang, J.; Peng, J.; Zhu, L.; et al. Design, Synthesis, and Biological Evaluation of Peptidomimetic Aldehydes as Broad-Spectrum Inhibitors against Enterovirus and SARS-CoV-2. *J. Med. Chem.* **2021**. [[CrossRef](#)]
101. Hamdy, R.; Fayed, B.; Mostafa, A.; Shama, N.M.A.; Mahmoud, S.H.; Mehta, C.H.; Nayak, Y.; Soliman, S.S.M. Iterated Virtual Screening-Assisted Antiviral and Enzyme Inhibition Assays Reveal the Discovery of Novel Promising Anti-SARS-CoV-2 with Dual Activity. *Int. J. Mol. Sci.* **2021**, *22*, 9057. [[CrossRef](#)]
102. Elseginy, S.A.; Fayed, B.; Hamdy, R.; Mahrous, N.; Mostafa, A.; Almehtdi, A.M.; Soliman, S.S.M. Promising anti-SARS-CoV-2 drugs by effective dual targeting against the viral and host proteases. *Bioorg. Med. Chem. Lett.* **2021**, *43*, 128099. [[CrossRef](#)]
103. Cui, J.; Jia, J. Discovery of juglone and its derivatives as potent SARS-CoV-2 main proteinase inhibitors. *Eur. J. Med. Chem.* **2021**, *225*, 113789. [[CrossRef](#)] [[PubMed](#)]
104. Hoffman, R.L.; Kania, R.S.; Brothers, M.A.; Davies, J.F.; Ferre, R.A.; Gajiwala, K.S.; He, M.; Hogan, R.J.; Kozminski, K.; Li, L.Y.; et al. Discovery of Ketone-Based Covalent Inhibitors of Coronavirus 3CL Proteases for the Potential Therapeutic Treatment of COVID-19. *J. Med. Chem.* **2020**, *63*, 12725–12747. [[CrossRef](#)] [[PubMed](#)]
105. Liu, C.; Boland, S.; Scholle, M.D.; Bardiot, D.; Marchand, A.; Chaltin, P.; Blatt, L.M.; Beigelman, L.; Symons, J.A.; Raboisson, P.; et al. Dual inhibition of SARS-CoV-2 and human rhinovirus with protease inhibitors in clinical development. *Antivir. Res.* **2021**, *187*, 105020. [[CrossRef](#)] [[PubMed](#)]
106. Vankadara, S.; Wong, Y.X.; Liu, B.; See, Y.Y.; Tan, L.H.; Tan, Q.W.; Wang, G.; Karuna, R.; Guo, X.; Tan, S.T.; et al. A head-to-head comparison of the inhibitory activities of 15 peptidomimetic SARS-CoV-2 3CLpro inhibitors. *Bioorg. Med. Chem. Lett.* **2021**, *48*, 128263. [[CrossRef](#)]
107. Owen, D.R.; Allerton, C.M.N.; Anderson, A.S.; Aschenbrenner, L.; Avery, M.; Berritt, S.; Boras, B.; Cardin, R.D.; Carlo, A.; Coffman, K.J.; et al. An oral SARS-CoV-2 M pro inhibitor clinical candidate for the treatment of COVID-19. *Science* **2021**, *374*, eabl4784. [[CrossRef](#)] [[PubMed](#)]
108. Sacco, M.D.; Ma, C.; Lagarias, P.; Gao, A.; Townsend, J.A.; Meng, X.; Dube, P.; Zhang, X.; Hu, Y.; Kitamura, N.; et al. Structure and inhibition of the SARS-CoV-2 main protease reveals strategy for developing dual inhibitors against M<sup>Pro</sup> and cathepsin L. *bioRxiv Prepr. Serv. Biol.* **2020**, *10*, 2020-07. [[CrossRef](#)]